molecules

MDPI

Article

Design, Synthesis and Cancer Cell Growth Inhibition Evaluation of New Aminoquinone Hybrid Molecules

Andrea Defant and Ines Mancini *

Laboratory of Bioorganic Chemistry, Department of Physics, University of Trento, Via Sommarive 14, 38123 Trento, Italy; andrea.defant@unitn.it

* Correspondence: ines.mancini@unitn.it; Tel.: +39-461-281-548

Academic Editors: Carla Boga and Gabriele Micheletti

Received: 4 June 2019; Accepted: 12 June 2019; Published: 14 June 2019

Abstract: Molecular hybridization has proven to be a successful multi-target strategy in the design and development of new antitumor agents. Based on this rational approach, we have planned hybrid molecules containing covalently linked pharmacophoric units, present individually in compounds acting as inhibitors of the cancer protein targets tubulin, human topoisomerase II and ROCK1. Seven new molecules, selected by docking calculation of the complexes with each of the proteins taken into consideration, have been efficiently synthesized starting from 2,3-dichloro-1,4-naphtoquinone or 6,7-dichloro-5,8-quinolinquinone. By screening the full National Cancer Institute (NCI) panel, including 60 human cancer cell lines, four molecules displayed good and sometimes better growth inhibition GI_{50} than the ROCK inhibitor Y-27632, the Topo II inhibitor podophyllotoxin and the tubulin inhibitor combretastatin A-4. The relative position of *N*,*N* heteroatoms in the structures of the tested compounds was crucial in affecting bioactivity and selectivity. Furthermore, compound **3** (2-(4-(2-hydroxyethyl)piperazin-1-yl)-3-(3,4,5-trimethoxyphenoxy)naphthalene-1,4-dione) emerged as the most active in the series, showing a potent and selective inhibition of breast cancer BT-549 cells (GI_{50} < 10 nM).

Keywords: hybrid molecules; quinolinequinones; naphtoquinones; 3,4,5-trimethoxyphenyl group; docking calculation; antitumor activity; cytotoxicity

1. Introduction

Cancer is one of the prominent causes of death worldwide, and there is an urgent need to introduce new therapeutic agents due to resistance and severe side effects shown by the currently available drugs. Using molecules to act on different tumor targets simultaneously has shown a higher therapeutic potential than single-target chemotherapy. In the recent rational design of anticancer drugs, molecular hybridization is a promising approach. A hybrid molecule usually contains two or more pharmacophore scaffolds present in single therapeutically active agents, connected together in a new single structure by covalent bonds. The selection of these moieties is based on the strategy of combining structures and pharmacological activities of known drugs and bioactive natural or synthetic compounds [1]. The aim of this strategy is to obtain new therapeutic agents that are able not only to reduce undesirable side effects of the parent drugs, but also to display a modified selectivity profile, a higher affinity and a better therapeutic effect than the administration of a combination of the single-target drugs [2]. Hybrid molecules have demonstrated more favorable pharmacokinetic and pharmacodynamic parameters, in addition to dual or multiple modes of action, due to their ability to inhibit more than one biological target [1]. It is therefore understandable that the investigation of new hybrid anticancer drugs has recently become of great therapeutic interest.

Tubulin is a protein composed of microtubules which are the main components of the cellular cytoskeleton. They play a pivotal role in proliferation, migration and mitosis. Molecules able to bind

this protein interfere with microtubule polymerization and depolymerization, inducing cell cycle arrest and leading to apoptosis in cancer cells. A variety of molecules have been proven to act efficiently as tubulin inhibitors, but their therapeutic use is limited by toxicity and development of resistance. Molecular hybridization has been used with good results to target this protein [3].

Topoisomerases (Topo I and Topo II) are enzymes that change the topological state of DNA through the breaking and rejoining of DNA strands. They have a relevant role in replication, recombination, transcription and preservation of genome stability. A series of currently used anticancer drugs and molecules in clinical trials act as inhibitors of these enzymes, stabilizing the DNA-Topo complex by intercalation between DNA base pairs. Therefore, inhibition of human topoisomerases is a promising target in the development of new antitumor agents [4].

Rho-associated kinases, known as two isoforms, ROCK1 and ROCK2, have been shown to induce stress fiber formation, cancer cell migration and metastasis. ROCK protein expression is elevated in several types of cancer. In a series of both in vitro and in vivo studies, advantages have been demonstrated by blocking these proteins, obtaining results especially in reducing tumor growth and in preventing metastases. The data support the potential of ROCKs as targets against tumors [5].

We report here on the efficient synthesis of seven new amino-quinone derivatives, designed as hybrid molecules that combine structural units present in inhibitors of tubulin, topoisomerase II and ROCK as tumor targets, and selected by docking calculations as ligands of these proteins. The evaluation on the growth inhibition of cancer cells by the in vitro NCI screening has been related to the structural features of these hybrid molecules.

2. Results and Discussion

2.1. In Silico Molecular Modeling

The 3,4,5-trimethoxyphenyl (TMP) unit is a structural feature of anti-neoplastic molecules. It is the case of the natural phenols combretastatins, whose biological activities have been attributed to the presence of this moiety's ability to target tubulin by the inhibition of microtubule formation. Other representative examples are given by colchicine and podophyllotoxin (Figure 1) [6], which make this pharmacophore a peculiar structural motif among the effective tubulin inhibitors studied in the last decades, with a special value in the design of new antitumor drugs. In addition, podophyllotoxin derivatives acting as topoisomerase II inhibitors are drugs commonly used in clinical oncology [7]. MPT0B214, also showing the TMP unit (Figure 1), inhibits tubulin polymerization and induces apoptosis through mitochondria-mediated pathways [8]. Naphthoquinone and quinolinequinones cores are other representative chemical scaffolds for the development of antitumor agents, which are present in structures of natural and synthetic bioactive products [9,10]. Their molecular mechanism includes reactive oxygen species (ROS) generation mediated by naphtoquinone oxidoreductase 1 (NQO1) bioreduction [11]. Quinolinequinone is a structural unit also present in 7-chloro-6-piperidinyl-quinoline-5,8-dione (PT-262, Figure 1), a synthetic molecule showing an effective inhibition of ROCK kinase activities [12].

Based on these evidences, the structures considered in this molecular hybridization design show a quinone unit with X, Y as CH or *N*, substituted by both a linear or cyclic amine and a 3,4,5 trimethoxyphenyl ether (Figure 1). A very good overlap has been observed for the energy-minimized structures of PT-262 and podophyllotoxin in cases where quinolinequinone is substituted by piperidine as a cyclic amine (corresponding to **1b** in Scheme 1) in the planned molecule, showing an *N*,*N*-anti configuration (as in PT-262 (Figure S1)).

In silico screening of the interactions with the target proteins tubulin, human topoisomerase II β and human ROCK1 (Table S1) via docking calculation permitted the selection of the new molecules **1a–c**, **2a–c** and **3** (Scheme 1). Their drug-likeness was computationally predicted regarding the physico-chemical properties relevant for the development of a drug. By using the free web tool SwissADME, a series of descriptors were calculated, taking into account lipophilicity, size, polarity,

solubility, flexibility and unsaturation [13]. All the designed molecules showed a behavior that respected the parameters necessary for good bioavailability (Table S2).

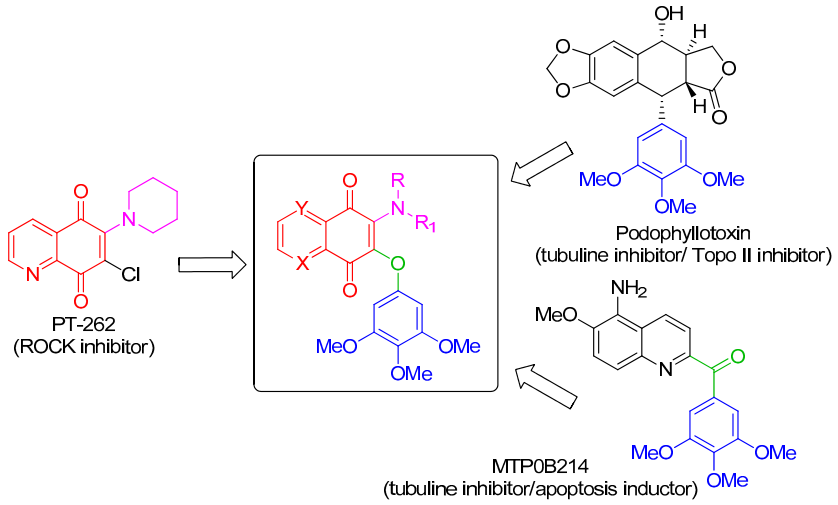

Figure 1. Design strategy of the target hybrid molecules.

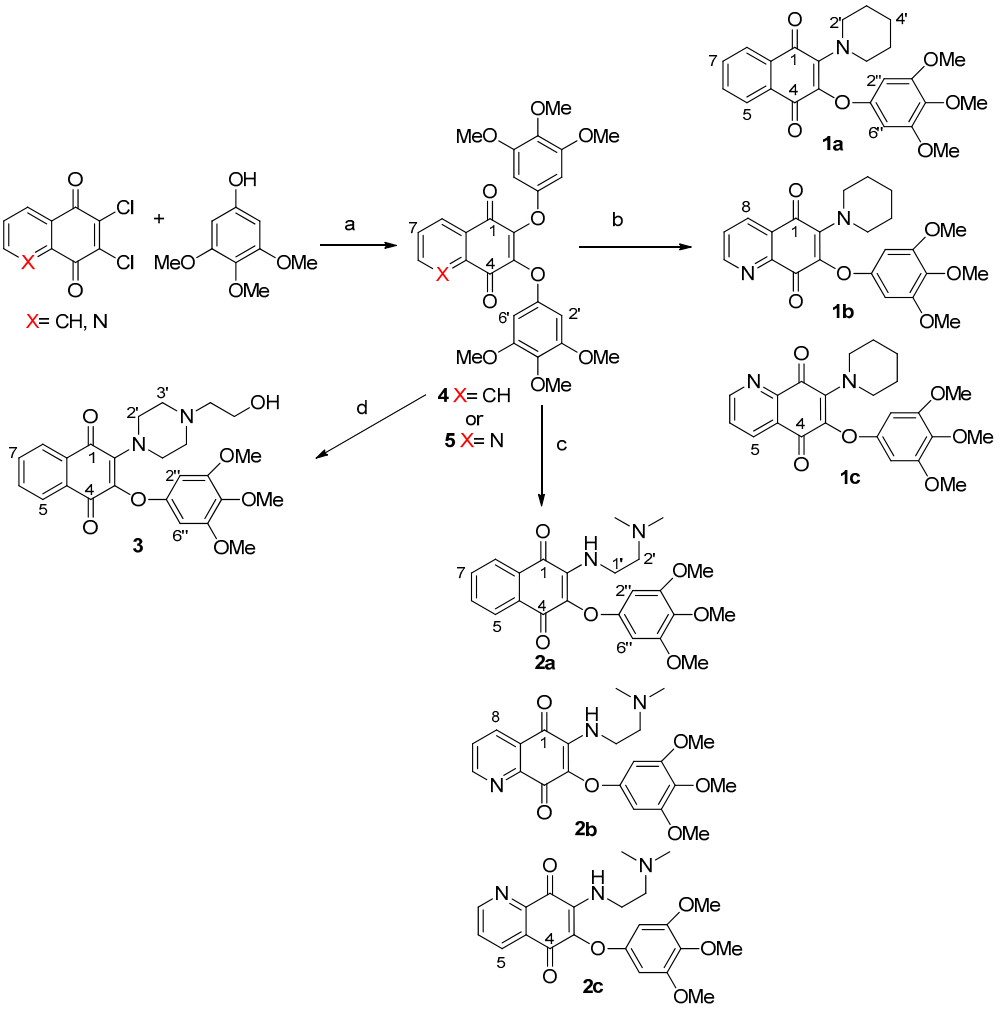

Scheme 1. Synthesis of molecules **1a–c, 3a–c** and **3.** Reagents and conditions: (**a**) K_2CO_3, DMSO, r.t. 48 h; (**b**) piperidine, CH_2Cl_2, r.t. 24 h; (**c**) *N1*,*N1*-dimethylethane-1,2-diamine, CH_2Cl_2, r.t. 24 h; (**d**) 2-(piperazin-1-yl)ethan-1-ol, CH_2Cl_2, r.t. 24 h. Arbitrary numbering is for convenience.

2.2. Synthesis of Compounds 1a–c, 2a–c and 3

The desired products were easily accessible using the common precursors **4** and **5**, by the reaction carried out at room temperature in DMSO in the presence of potassium carbonate of 3,4,5-trimethoxyphenol with 2,3-dicholoro-1,4-naphtoquinone or 6,7-dichloro-5,8-quinolinequinone respectively (Scheme 1), via a proposed mechanism involving a Michael addition followed by chloride elimination [14]. The following treatment of compound **4** with piperidine, *N*,*N*dimethylethane-1,2 diamine or 2-(piperazin-1-yl)ethan-1-ol in dichloromethane at room temperature provided the products **1a**, **2a** and **3**, respectively, with global yields in the range 77% ÷ 79%, as evaluated after chromatographic purification of the products. It has been reported that similar quinones with one chlorine and one alkoxyl unit preferentially react by replacing the latter group [15,16], and therefore the use of the symmetric disubstituted 3,4,5-trimethoxyphenoxyl reagent was essential. Through a similar procedure, the products **1b**, **1c**, **2b** and **2c** were obtained starting from the quinolinequinone **5**. Pure regioisomers **1b** and **1c** with a 40:60 ratio resulted from chromatographic separation on silica gel by elution with dichloromethane/methanol/triethylamine 95:5:0.1. Similarly, **2b** and **2c** were isolated in a 42:58 ratio. Structural assignments of the regioisomer pairs **1b**/**2b** and **1c**/**2c** were based on long-range hetero-correlations observed by HMBC experiments. In detail, taking as references the data obtained for similar isomers [17]: (*i*) $^{3}J(^{1}H, ^{13}C)$ couplings of the signal at 8.35 ppm for H-8 with 183.2 ppm for C(1)=O in **1b**, and 8.36 ppm with 182.0 ppm for **2b**, supported the *N*,*N*-anti configuration; (*ii*) $^{3}J(^{1}H, ^{13}C)$ couplings of the signal at 8.34 ppm for H-5 with 177.1 ppm for C(1)=O in **1c**, and 8.38 ppm with 176.3 ppm for **2c**, supported the *N*,*N*-syn configuration (Scheme 1).

2.3. Biological Evaluation

Compounds **1a**–**c**, **2a**–**c** and **3** were subjected to in vitro growth percentage activity on the NCI full panel containing 60 human cancer cell lines at a single dose at 10 μM. From this evaluation compounds **1a**, **1c** and **2a** were considered inactive (Table 1), whereas **1b**, **2b**, **2c** and **3** were selected for further investigation at five concentration levels. Table 2 reports GI_{50} data (defined as the concentration values of the molecules inhibiting the growth of cancer cells by 50%) in comparison with the values reported in the NCI database for the ROCK inhibitor Y-27632, the Topo II inhibitor podophyllotoxin and the tubulin inhibitor combretastatin A-4 [18]. The GI_{50} values of the new tested compounds resulted in 10 nM ÷ 10 μM range.

Table 1. Mean dose percent values by one-dose assay (10^{-5} M) of all the tested compounds in the full NCI 60 cell panel.

Compound	Mean Growth Percent	Activity
1a	93.74	Inactive
1b	20.92	Active
1c	67.49	Inactive
2a	78.44	Inactive
2b	−4.33	Active
2c	12.79	Active
3	17.88	Active

Table 2. Inhibition of in vitro human cancer cell lines by compounds **1a**, **2b**, **2c** and **3**, in comparison with combretastatin A-4, podophyllotoxin and Y-27632 taken as reference compounds.

	Cytotoxicity GI_{50} (μM)						
	1b	**2b**	**2c**	**3**	**Y-27632**	**Podophyllotoxin**	**Combretastatin A-4**
Cell lines							
Leukemia							
CCRF-CEM	2.98	2.21	2.24	2.48	31.6	0.01	0.251
HL-60(TB)	1.76	0.811	1.43	1.66	100	0.01	0.01
K-562	0.354	0.659	2.90	2.19	100	-	0.316
MOLT-4	3.58	3.07	2.48	2.35	100	0.01	0.501
RPMI-8226	0.486	1.92	2.23	2.03	100	0.01	0.063
SR	1.89	3.17	2.13	2.87	25.1	0.01	1.99
Non-Small Cell Lung Cancer							
A549/ATCC	0.482	3.43	1.87	13.8	100	0.0126	0.020
HOP-92	10.4	1.88	2.01	1.46	1.26	0.0316	0.100
NCI-H226	0.506	16.67	2.08	2.92	100	0.01	0.251
NCI-H23	2.11	2.25	1.76	2.22	100	0.01	0.040
NCI-H322M	6.27	2.65	7.04	1.23	100	0.01	0.063
NCI-H460	2.77	3.11	1.65	3.13	100	0.01	0.050
NCI-H522	1.47	1.46	1.39	0.571	100	0.01	0.032
Colon Cancer							
COLO 205	2.79	1.10	2.44	1.80	100	0.01	6.31
HCC-2998	5.57	1.62	4.71	12.4	100	0.0126	0.158
HCT-116	0.513	0.277	1.85	1.44	100	0.01	0.079
HCT-15	0.442	2.07	2.78	1.56	100	0.0126	0.040
HT29	3.74	2.36	3.77	2.27	100	0.01	6.31
KM12	4.59	2.91	3.34	4.39	100	0.01	0.063
SW-620	1.37	0.318	1.55	1.79	100	0.01	0.063
CNS Cancer							
SF-268	1.94	2.39	2.87	1.73	63.1	0.01	0.063
SF-295	0.465	9.88	3.76	5.36	100	0.01	0.032
SF-539	0.434	1.78	1.85	2.48	100	0.01	0.025
SNB-19	0.450	2.00	2.86	3.41	100	0.01	0.025
SNB-75	0.334	1.89	1.39	1.68	10	0.01	1.259
U251	0.440	2.00	2.12	3.10	100	0.01	0.079
Melanoma							
LOX IMVI	1.01	0.508	1.76	1.81	100	0.01	0.050
MALME-3M	2.73	0.967	2.23	3.99	100	50.1	0.631
M14	0.552	1.84	3.07	1.96	100	0.0126	0.100
MDA-MB-435	1.11	1.72	1.53	1.76	100	0.01	0.010
SK-MEL-2	4.16	2.03	2.01	2.01	100	0.016	0.050
SK-MEL-28	1.35	-	2.00	2.34	100	0.01	5.012
SK-MEL-5	1.95	1.70	1.55	1.81	100	0.01	0.013
UACC-257	0.846	1.78	1.56	3.56	100	0.01	0.063
UACC-62	2.53	3.17	1.60	1.79	100	0.01	0.040
Ovarian Cancer							
OVCAR-3	1.77	0.364	2.02	1.02	79.4	0.0126	0.051
OVCAR-4	1.31	0.937	1.53	1.63	100	0.016	1.995
OVCAR-5	0.439	2.35	2.19	2.60	100	0.251	3.981
OVCAR-8	0.463	0.386	2.13	2.91	100	0.01	0.079
NCI/ADR-RES	1.06	7.40	5.95	3.19	100	0.01	0.063
SK-OV-3	3.28	11.6	7.49	5.31	100	0.01	0.251
Renal Cancer							
786-0	2.03	2.46	2.04	1.93	100	0.016	0.631
A498	0.640	2.17	2.09	2.04	100	0.01	0.100
ACHN	1.25	1.81	2.36	1.87	100	0.01	0.199
CAKI-1	0.595	2.10	2.51	3.59	100	0.1	0.251
RXF 393	0.694	2.00	2.83	1.55	100	0.01	0.398
SN12C	0.829	2.81	2.02	3.11	100	0.016	0.251
TK-10	3.27	3.63	3.91	4.97	10	0.0316	3.162
UO-31	1.18	1.80	1.29	1.61	100	0.016	1.000
Prostate Cancer							
PC-3	0.914	2.43	2.72	3.19	100	0.01	0.010
DU-145	2.60	3.43	4.19	-	100	0.01	0.013

Table 2. *Cont.*

	Cytotoxicity GI_{50} (μM)						
	1b	**2b**	**2c**	**3**	**Y-27632**	**Podophyllotoxin**	**Combretastatin A-4**
Breast Cancer							
MCF7	0.509	0.304	1.20	1.15	100	0.01	0.010
MDA-MB-231/ATCC	4.14	2.55	1.81	2.00	100	0.01	0.016
HS 578T	0.415	3.06	2.84	2.69	100	0.01	0.010
BT-549	0.819	2.68	4.96	<0.01	100	0.01	0.020
T-47D	2.53	1.67	1.98	0.510	100	79.4	50.12
MDA-MB-468	1.77	0.133	0.285	1.37	100	0.01	0.079
MGM [a)]	1.29	1.82	2.24	2.24	91.6	1.52	1.52

[a)] MGM (mean graph medium) value as average GI50 (μM) over all cell lines investigated.

Submicromolar activities were observed for compound **1b** (Table 2), in particular against central nervous system (CNS) cancer for most of the tested cell lines (Figure 2a). Compound **2b** showed the highest inhibitions on MDA-MB-468 breast cancer cells (GI_{50} = 0.133 μM) and on both HCT-116 and SW-620 colon cell lines (GI_{50} 0.277 and 0.318 μM, respectively, Table 2). Notably, the relative structural position of *N*,*N* heteroatoms is crucial in affecting bioactivity and selectivity. In fact, compared with **2b**, its *N*,*N*-syn regioisomer **2c** displayed a lower activity corresponding to a growth inhibition in the micromolar range on the same cancer cell lines. A more pronounced disparity was observed for the pair **1b**/**1c**, where the *N*,*N*-syn isomer **1c** showed no activity. This is evident taking into account the values observed for all the synthesized compounds reported in Table 1 when expressed as the mean dose percentage of single high doses (10^{-5} M) from the full NCI 60 cell panel. Moreover, the structures lacking of the N atom on quinone unit as 1a and 2a provided inactive compounds (Table 1), whereas product 3 having additional heteroatoms on the C-2 substituent (specifically an NCH_2CH_2OH moiety) when compared with the inactive 1a, emerged as the most active molecule. Product **3** displayed submicromolar inhibition and was about 160 and 100 times more active than podophyllotoxin and combretastatin A-4, respectively, on T-47D breast cancer lines (Table 2). Furthermore, **3** emerged as the most promising in the series, with a selective GI_{50} value lower than 10 nM on BT-549 breast cancer cell line (Figure 2b).

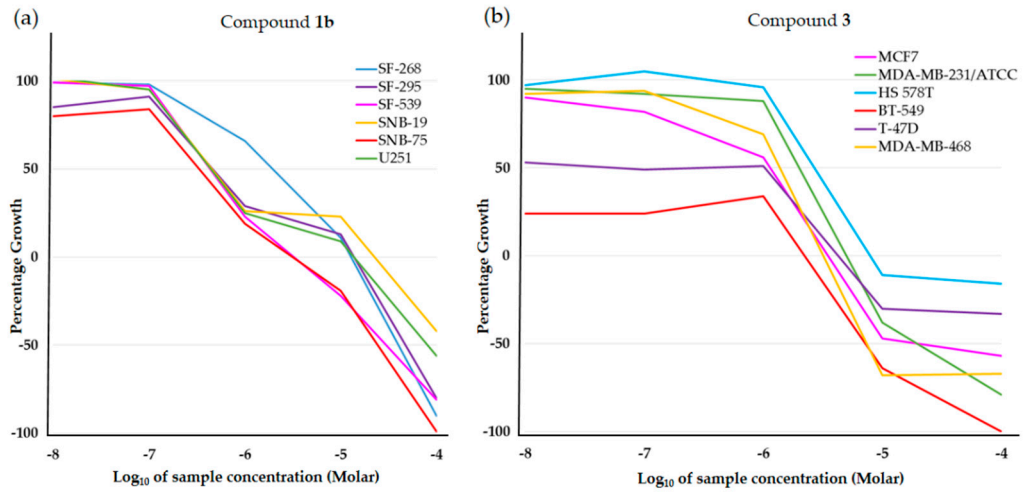

Figure 2. Dose response curves at NCI fixed protocol: (**a**) for compound **1b** on the indicated central nervous system (CNS) cancer cell lines, and (**b**) for compound **3** on the indicated breast cancer cell lines. The curves were obtained at five concentrations (log dilutions from 10^{-4} to 10^{-8} M). The concentrations of each compound, which inhibited 50% of cancer cell growth (GI_{50}), were deduced and are the values reported in Table 1.

3. Materials and Methods

3.1. Chemistry

3.1.1. General

All reagents were purchased from Sigma Aldrich and used without further purification. Preparation of 6,7-Dichloroquinoline-5,8-dione followed a reported procedure [14,19]. The reaction yields were calculated for the products after chromatographic purification. Thin layer chromatography (TLC): Merck silica gel F_{254} or reversed phase Merck RP-18 F_{254}, with visualization using UV light. Flash chromatography (FC): Merck Si 15–25 μm. Preparative thin layer chromatography (PLC): 20 × 20 cm Merck Kieselgel 60 F_{254} 0.5-mm plates. NMR spectra were recorded on a Bruker-Avance 400 spectrometer using a 5-mm BBI probe ^{1}H at 400 MHz and ^{13}C at 100 MHz in $CDCl_3$ (relative to δ_H 7.25 and δ_C 77.00 ppm), with δ values in ppm and *J* values in Hz; assignments were supported by heteronuclear single quantum correlation (HSQC) and heteronuclear multiple bond correlation (HMBC) experiments. Electrospray ionization (ESI)-MS mass spectra were recorded using a Bruker Esquire-LC spectrometer by direct infusion of a methanol solution (source temperature 300 °C, drying gas N_2, 4 L min^{-1}, scan range *m/z* 100 ÷ 1000). Electron ionization (EI) mass spectra (*m/z*; rel%) and high resolution (HR)-EI data were recorded with a Kratos-MS80 mass spectrometer, heating at 213 °C for **2a**–**c**, at 276 °C for **1a**–**c** and at 417 °C for compound **3**, using a home-built computerized acquisition software.

3.1.2. Typical Reaction Procedure for Precursors **4** and **5**

Anhydrous potassium carbonate (414 mg, 3.00 mmol, 1.5 equiv) was added to a solution of 2,3-dichloro-1,4-naphtoquinone (227 mg, 1.00 mmol, 1.0 equiv) or 6,7-dichloro-5,8-quinolinquinone (228 mg, 1.00 mmol, 1.0 equiv) and 3,4,5-trimethoxyphenol (384 mg, 2.00 mmol, 2.00 equiv) in 2.5 mL of dry DMSO, and the reaction mixture was stirred at room temperature for 48 h. The mixture was decanted to remove inorganic salt, and partitioned between dichloromethane/water (X3). The combined organic extracts were washed with water, dried over anhydrous Na_2SO_4 and concentrated in vacuo to give a solid that was purified by silica gel FC eluting with hexane/EtOAc (from 9:1 to 6:4 v/v) for **4,** and with dichloromethane/methanol/triethylamine (96:4:0.1 v/v) for **5.**

2,3-Bis(3,4,5-trimethoxyphenoxy)naphthalene-1,4-dione (**4**). TLC (hexane: EtOAc = 1:1 v/v): R_f = 0.50. Light orange solid. Yield: 87%. ^{1}H-NMR (400 MHz, $CDCl_3$) δ 8.15 and 7.79 (two m, 2H each, H-5/H-8 and H-6/H-7), 6.11 (s, 4H, H-2′, H-6′, H-2′and H-6′), 3.75 (s, 6H, -OCH_3), 3.72 (s, 12H, -OCH_3). ^{13}C-NMR (100 MHz, $CDCl_3$) δ 180.4 (C=O), 153.7, 134.7, 134.5, 130.7, 126.5, 94.4, 60.7 (-OCH_3), 56.0(-OCH_3). Significant HMBC correlations: 8.15 ppm with 180.4 ppm; 7.79 ppm with 130.7 ppm. ESI(+)-MS: *m/z* 545 $[M + Na]^+$. HRMS(EI) calcd. for $C_{28}H_{26}O_{10}$, 522.15260, found 522.15248.

6,7-Bis(3,4,5-trimethoxyphenoxy)quinoline-5,8-dione (**5**). TLC (CH_2Cl_2/MeOH = 95:5 v/v, with two drops of Et_3N): R_f = 0.90. Brown solid. Yield: 93%. ^{1}H-NMR (400 MHz, $CDCl_3$) δ 9.11 (br d, *J* = 4.9 Hz, 1H, H-6), 8.49 (d, *J* = 7.5 Hz, 1H, H-8), 7.75 (dd, *J* = 7.5, 4.9 Hz 1H, H-7), 6.12 and 6.08 (two s, 2H each, H-2′, H-6′, H-2′and H-6′), 3.76 (s, 6H, -OCH_3), 3.73 (s, 12H, -OCH_3). ^{13}C-NMR (100 MHz, $CDCl_3$) δ 179.7 (C=O), 178.8 (C=O), 153.6, 153.5, 152.4, 146.7, 144.7, 135.5, 134.6, 127.8, 127.7, 94.0, 60.2 (-OCH_3), 55.5 (-OCH_3). Significant HMBC correlations: 9.11 ppm with 146.7 ppm; 8.49 ppm with 179.7 ppm; 7.75 ppm with 127.7 ppm; 6.12 and 6.10 ppm with 152.4, 146.7 and 134.6 ppm; 3.76 ppm with 134.6 ppm; 3.73 ppm with 152.4 ppm ESI(+)-MS: *m/z* 524 $[M + H]^+$, 545 $[M + Na]^+$, 562 $[M + K]^+$. HRMS(EI) calcd. for $C_{27}H_{25}NO_{10}$, 523.14785, found 523.14778.

3.1.3. Typical Reaction Procedure for the Synthesis of Compounds **1a**–**c**, **2a**–**c** and **3**

A mixture of compound **4** or **5** (52.2 mg, 0.10 mmol, 1.0 equiv) and the suitable amine (0.20 mmol, 2.0 equiv) in 2 mL of anhydrous dichloromethane was stirred at room temperature for 24 h. The solvent

was removed in vacuo and the residue was purified by PLC eluting with hexane/EtOAc 1:1 (v/v) for **1a** and CH_2Cl_2/MeOH/Et_3N 95:5:0.1 (v/v) for the other compounds.

2-(Piperidin-1-yl)-3-(3,4,5-trimethoxyphenoxy)naphthalene-1,4-dione (**1a**). TLC (hexane: EtOAc = 1:1 v/v): Rf = 0.74. Red solid. Yield: 91%. ^{1}H-NMR (400 MHz, $CDCl_3$) δ 8.02 and 7.65 (two m, 2H each, H-5/H-8 and H-6/H-7), 6.18 (s, 2H, H-2′ and H-6′), 3.77 (s, 9H, three –OCH_3), 3.43 (br s, 4H, H-2′and H-6′), 1.65 (br s, 6H, H-3′, H-4′and H-5′). ^{13}C-NMR (100 MHz, $CDCl_3$) δ 184.1 and 178.4 (two C=O), 154.3, 142.2, 134.2, 133.3, 132.3, 126.2, 96.2, 56.2 (-OCH_3), 51.4, 28.2. Significant HMBC correlations: 8.02 ppm with 184.1 and 178.4 ppm; 7.65 ppm with 132.3 ppm. ESI(+)-MS: *m/z* 462 $[M + K]^+$, 446$[M + Na]^+$, 424 $[M + H]^+$. HRMS(EI) calcd. for $C_{24}H_{25}NO_6$, 423.16819, found 423.16810.

6-(Piperidin-1-yl)-7-(3,4,5-trimethoxyphenoxy)quinoline-5,8-dione (**1b**). TLC (CH_2Cl_2/MeOH = 95:5 v/v, with two drops of Et_3N): R_f = 0.93. Violet solid. Yield: 40% (as single regioisomer). ^{1}H-NMR (400 MHz, $CDCl_3$) δ 8.97 (br d, *J* = 4.9 Hz, 1H, H-6), 8.35 (br d, *J* = 7.9 Hz, 1H, H-8), 7.59 (m, 1H, H-7), 6.20 (s, 2H, H-2′ and H-6′), 3.79 and 3.77 (two s, 9H, OCH_3), 3.45 (m, 4H, H-2′ and H-6′), 1.65 (m, 6H, H-3′, H-4′and H-5′). ^{13}C-NMR (100 MHz, $CDCl_3$) δ 183.2 (C=O), 154.9, 154.0, 147.3, 145.4, 139.7, 135.7, 133.7, 128.5, 126.1, 91.8, 56.7, 51.4, 29.2, 24.0. Significant HMBC correlations: 8.35 ppm with 183.2 and 128.5 ppm; 7.59 ppm with 128.5 ppm; 6.20 ppm with 139.8 ppm; 3.45 ppm with 145.4 and 29.2 ppm. ESI(+)-MS: *m/z* 447 $[M + Na]^+$. HRMS(EI) calcd. for $C_{23}H_{24}N_2O_6$, 424.16344, found 424.16329.

7-(Piperidin-1-yl)-6-(3,4,5-trimethoxyphenoxy)quinoline-5,8-dione (**1c**). TLC (CH_2Cl_2/MeOH = 95:5 v/v, with two drops of Et_3N): R_f = 0.90. Violet solid. Yield: 60% (as single regioisomer). ^{1}H-NMR (400 MHz, $CDCl_3$) δ 8.93 (br d, *J* = 4.8 Hz, 1H, H-7), 8.34 (br d, *J* = 7.9 Hz, 1H, H-5), 7.61 (m, 1H, H-6), 6.19 (s, 2H, H-2′ and H-6′), 3.78 (s, 9H, OCH_3), 3.50 (br s, 4H, H-2′ and H-6′), 1.69 (m, 6H, H-3′, H-4′ and H-5′). ^{13}C-NMR (100 MHz, $CDCl_3$) δ 182.4 and 177.1 (two C=O), 154.4 154.1, 151.6, 151.1, 147.7, 134.2, 133.5, 127.9, 92.9, 56.2, 52.6, 26.9, 25.0. Significant HMBC correlations: 8.93 ppm with 151.1 and 127.9 ppm; 8.34 ppm with 177.1 and 151.1 ppm; 7.61 ppm with 154.4 ppm; 6.19 ppm with 154.1 and 133.5 ppm. ESI(+)-MS: *m/z* 463 $[M + K]^+$, 447 $[M + Na]^+$, 425 $[M + H]^+$. HRMS(EI) calcd. for $C_{23}H_{24}N_2O_6$, 424.16344, found 424.16328.

2-((2-(Dimethylamino)ethyl)amino)-3-(3,4,5-trimethoxyphenoxy)naphthalene-1,4-dione (**2a**). TLC (CH_2Cl_2/MeOH = 95:5 v/v, with two drops of Et_3N): R_f = 0.30. Orange solid. Yield: 90%. ^{1}H-NMR (400 MHz, $CDCl_3$) δ 8.05 (d, *J* = 7.5 Hz, 2H, H-5 and H-8), 7.70 and 7.61 (two t, *J* = 7.7 Hz, 2H, H-6 and H-7), 6.40 (br s, 1H, *N*H), 6.22 (s, 2H, H-2′ and H-6′), 3.77 (s, 6H, two –OCH_3), 3.75 (s, 3H, –OCH_3), 3.56 (q, *J* = 5.5 Hz, 2H, H-1′), 2.49 (t, *J* = 5.5 Hz, 2H, H-2′), 2.22 (s, 6H, $N(CH_3)_2$). ^{13}C-NMR (100 MHz, $CDCl_3$) δ 182.4 and 177.8 (C=O), 155.1, 134.2, 133.3, 132.1, 129.8, 126.4, 92.6, 58.9 (C-2′), 55.9 (-OCH_3), 44.6 (*N*$(CH_3)_2$), 41.7 (C-1′). Significant HMBC correlations: 8.05 ppm with 182.4 and 177.8 ppm; 7.65 ppm with 132.3 ppm; 7.70 ppm with 134.2 ppm; 7.61 ppm with 132.1 ppm; 6.22 ppm with 155.1 and 133.3 ppm. ESI(+)-MS: *m/z* 449 $[M + Na]^+$, 427 $[M + H]^+$. HRMS(EI) calcd. for $C_{23}H_{26}N_2O_6$, 426.17909, found 426.17896.

6-((2-(Dimethylamino)ethyl)amino)-7-(3,4,5-trimethoxyphenoxy)quinoline-5,8-dione (**2b**). TLC (CH_2Cl_2/MeOH = 95:5 v/v, with two drops of Et_3N): R_f = 0.28. Orange solid. Yield: 42% (as single regioisomer). ^{1}H-NMR (400 MHz, $CDCl_3$) δ 8.99 (br d, *J* = 4.8 Hz, 1H, H-6), 8.36 (br d, *J* = 7.9 Hz, 1H, H-8), 7.55 (dd, *J* = 7.9, 4.8 Hz, 1H, H-7), 6.46 (br s, 1H, NH), 6.23 (s, 2H, H-2′and H-6′), 3.78 and 3.77 (two s, 9H, three –OCH_3), 3.57 (m, 2H, H-1′), 2.49 (br t, *J* = 5.3 Hz, 2H, H-2′,), 2.22 (s, 6H, *N*$(CH_3)_2$). ^{13}C-NMR (100 MHz,$CDCl_3$) δ 182.0 (C=O), 176.1 (C=O), 154.6, 154.4, 148.6, 136.9, 133.7, 130.1, 123.8, 93.2, 57.8 (-OCH_3), 57.7 (C-2′), 44.5 (-*N*$(CH_3)_2$), 41.1(C-1′). Significant HMBC correlations: 8.99 ppm with 123.8 ppm; 8.36 ppm with 182.0, 154.4 and 148.6 ppm; 7.55 ppm with 154.4 and 130.1 ppm; 6.24 ppm with 154.6 and 133.7 ppm; 3.78 and 3.77 ppm with 154.6 and 133.7 ppm; 2.49 ppm with 41.1 ppm; 2.23 ppm with 57.7 ppm. ESI(+)-MS: *m/z* 450 $[M + Na]^+$, 428 $[M + H]^+$. HRMS(EI) calcd. for $C_{22}H_{25}N_3O_6$, 427.17434, found 427.17446.

7-((2-(Dimethylamino)ethyl)amino)-6-(3,4,5-trimethoxyphenoxy)quinoline-5,8-dione (**2c**). TLC (CH_2Cl_2/MeOH = 95:5 v/v, with two drops of Et_3N): R_f = 0.31. Orange solid. Yield: 58% (as single regioisomer).

^{1}H-NMR (400 MHz, $CDCl_3$) δ 8.92 (br d, *J* = 4.6 Hz, 1H, H-7), 8.38 (br d, *J* = 7.9 Hz, 1H, H-5), 7.62 (dd, *J* = 7.8, 4.5 Hz, 1H, H-6), 6.53 (br s, 1H, NH), 6.22 (s, 2H, H-2′ and H-6′), 3.78 (s, 9H, three –OCH_3), 3.61 (m, 2H, H-1′), 2.50 (br t, *J* = 5.7 Hz, 2H, H-2′), 2.22 (s, 6H, *N*$(CH_3)_2$). ^{13}C-NMR (100 MHz, $CDCl_3$) δ 180.9 (C=O), 176.3 (C=O), 155.0, 153.2, 151.4, 147.2, 135.1, 133.6, 132.2, 127.0, 93.2, 58.5 (C-2′), 56.5 (-OCH_3), 44.7 (-*N*$(CH_3)_2$), 41.2 (C-1′). Significant HMBC correlations: 8.92 ppm with 147.2, 135.1 and 127.0 ppm; 8.38 ppm with 180.9 (small), 176.3, 153.2 and 147.2 ppm; 7.62 ppm with 153.2, 135.1 and 132.2 ppm; 6.22 ppm with 155.0 and 133.6 ppm; 3.78 ppm with 155.0 and 133.6 ppm. ESI(+)-MS: *m/z* 450 $[M + Na]^+$. HRMS(EI) calcd. for $C_{22}H_{25}N_3O_6$, 427.17434, found 427.17427.

2-(4-(2-Hydroxyethyl)piperazin-1-yl)-3-(3,4,5-trimethoxyphenoxy)naphthalene-1,4-dione (**3**). TLC (CH_2Cl_2/MeOH = 95:5 v/v, with two drops of Et_3N): R_f = 0.30. Red solid. Yield: 88%. ^{1}H-NMR (400 MHz, $CDCl_3$) δ 8.01 and 7.66 (two m, 2H each, H-5/H-8 and H-6/H-7), 6.17 (s, 2H, H-2′ and H-6′), 3.77 (s, 9H, OCH_3), 3.60 (m, 2H, CH_2OH), 3.52 (m, 4H, H-2′), 2.59 (m, 4H, H-2′), 2.54 (m, 2H, *N*CH_2). ^{13}C-NMR (100 MHz, $CDCl_3$) δ 183.7 and 178.6 (C=O), 154.0, 133.6, 133.5, 132.3, 131.7, 126.2, 92.6, 56.6, 55.9 (OCH_3), 54.2, 49.8. Significant HMBC correlations: 8.01 ppm with 183.7 and 178.6 ppm; 7.66 ppm with 132.3 and 131.7 ppm; 6.17 ppm with 154.0 and 133.5 ppm. ESI(+)-MS: *m/z* 491 $[M + Na]^+$, 469 $[M + H]^+$. HRMS(EI) calcd. for $C_{25}H_{28}N_2O_7$, 468.18965, found 468.18951.

3.2. Computational Analysis

Calculations were carried out using Autodock Vina 1.1.2 [20], adopting a reported procedure [21]. The structures of human ROCK 1 (PDB ID: 2ETK), human topoisomerase II β (PDB ID: 3QX3) and tubulin (PDB ID: 5JCB) were determined by X-ray crystallography with a resolution of 2.9, 2.2 and 2.3 Å respectively. For the docking calculation, a grid box of 16 × 16 × 24 Å in x, y, z directions was created with a spacing of 1.00 Å, and centered at x = 51.964, y = 101.296, z = 29.213 for 2ETK; a grid box of 22 × 18 × 18 Å in x, y, z directions was created with a spacing of 1.00 Å, and centered at x = 32.884, y = 95.413, z = 50.785 for 3QX3; and a grid box of 18 × 28 × 26 Å in x, y, z directions was created with a spacing of 1.00 Å, centered at x = −13.614, y = 9.720, z = 20.911 for 5JCB. Results were expressed as energy associated to each ligand–enzyme complex in terms of Gibbs free energy values (Table S1). The visual ligand–enzyme interactions were displayed using Discovery Studio Visualizer v.19.1.0.18287 [22]. ADME predictions were performed using the online server Swiss-ADME [23].

3.3. Biological Evaluation

The synthesized compounds were evaluated for their in vitro activity against cancer cell lines by the National Cancer Institute (NCI-USA) following its anticancer drug development program based on automated sulforhodamine blue (SRB) cytotoxicity assay. The screening was a two-stage process, where after a first evaluation was carried out against the full panel of cell lines at a single dose of 10 μM, with the compounds exhibiting significant growth inhibition being tested at five concentration levels [24].

4. Conclusions

Based on the known benefits of considering a molecular hybridization approach in the design and development of new antitumor agents, we have planned new hybrid molecules containing pharmacophoric units, which present individually in compounds acting as inhibitors of the cancer protein targets tubulin, human topoisomerase II and ROCK1. Docking calculation of the complexes with each protein allowed us to select seven molecules, structurally characterized by a naphtoquinone or quinolinequinone moiety, and substituted by both a cyclic or functionalized amine and a 3,4,5-trimethoxyphenyl group.

The evaluation of human cancer cell inhibition by the seven synthetic compounds provided a qualitative structure–activity relationship study. What is more, compound **3** emerged as the most active in the series, displaying a selective nanomolar inhibition of breast cancer BT-549 cells. According

to these promising findings and their easily accessible synthesis, the molecules herein reported are worthy of further biological investigation.

Supplementary Materials: The following are available online. Table S1: Energy data from docking calculation by Autodock Vina for **1a–c**, **2a–c** and **3**, in comparison with original and reference ligands; Table S2: ADME prediction of **1a–c**, **2a–c**, **3** and reference compounds evaluated by on-line Server Swiss-ADME; Figure S1: Overlapping of the energy minimized structures **1b**, PT-262 and podophyllotoxin; Figures S2–S23: NMR spectra of compounds **1a–c**, **2a–c**, **3**, **4** and **5**.

Author Contributions: Conceptualization, A.D.; software, A.D.; investigation, A.D.; writing—original draft preparation, A.D and I.M.; writing—review and editing, I.M.; supervision, I.M.; funding acquisition, I.M.

Funding: This research received no external funding.

Acknowledgments: The authors thank the National Cancer Institute (NCI) at Bethesda, USA for the antitumor screening tests of the compounds. We are grateful to Adriano Sterni, university of Trento for mass spectra recording.

Conflicts of Interest: The authors declare no conflict of interest.

References

1. Abbot, V.; Sharma, P.; Dhiman, S.; Noolvi, M.N.; Patel, H.M.; Bhardwaj, V. Small hybrid heteroaromatics: Resourceful biological tools in cancer research. *RSC Adv.* **2017**, *7*, 28313–28349. [CrossRef]
2. Kerru, N.; Singh, P.; Koorbanally, N.; Raj, R.; Kumar, V. Recent advances (2015–2016) in anticancer hybrids. *Eur. J. Med. Chem.* **2017**, *142*, 179–212. [CrossRef] [PubMed]
3. Nepali, K.; Sharma, S.; Sharma, M.; Bedi, P.M.; Dhar, K.L. Rational approaches, design strategies, structure activity relationship and mechanistic insights for anticancer hybrids. *Eur. J. Med. Chem.* **2014**, *77*, 422–487. [CrossRef] [PubMed]
4. Pommier, Y.; Sun, Y.; Huang, S.N.; Nitiss, J.L. Roles of eukaryotic topoisomerases in transcription, replication and genomic stability. *Nat. Rev. Mol. Cell Biol.* **2016**, *17*, 703–721. [CrossRef] [PubMed]
5. Morgan-Fisher, M.; Wewer, U.M.; Yoneda, A. Regulation of ROCK activity in cancer. *J. Histochem. Cytochem.* **2013**, *61*, 185–198. [CrossRef] [PubMed]
6. Li, L.; Jiang, S.; Li, X.; Liu, Y.; Su, J.; Chen, J. Recent advances in trimethoxyphenyl (TMP) based tubulin inhibitors targeting the colchicine binding site. *Eur. J. Med. Chem.* **2018**, *151*, 482–494. [CrossRef] [PubMed]
7. Hartmann, J.T.; Li, H.P. Camptothecin and podophyllotoxin derivatives inhibitors of topoisomerase I and II—Mechanisms of Action, Pharmacokinetics and Toxicity Profile. *Drug Saf.* **2006**, *29*, 209–230. [CrossRef] [PubMed]
8. Chiang, N.J.; Lin, C.I.; Liou, J.P.; Kuo, C.C.; Chang, C.Y.; Chen, L.T.; Chang, J.Y. A novel synthetic microtubule inhibitor, mpt0b214 exhibits antitumor activity in human tumor cells through mitochondria-dependent intrinsic pathway. *PLoS ONE* **2013**, *8*, e58953. [CrossRef] [PubMed]
9. Defant, A.; Guella, G.; Mancini, I. Synthesis and in vitro cytotoxicity evaluation of novel naphthindolizinedione derivatives. *Arch. Pharm. Chem. Life Sci.* **2007**, *340*, 147–153. [CrossRef] [PubMed]
10. Defant, A.; Guella, G.; Mancini, I. Synthesis and *in-vitro* cytotoxicity evaluation of novel naphtindolizinedione derivatives, part II: Improved activity for aza-analogues. *Arch. Pharm. Chem. Life Sci.* **2009**, *342*, 80–86. [CrossRef] [PubMed]
11. Qiu, H.Y.; Wang, P.F.; Lin, H.Y.; Tang, C.Y.; Zhu, H.L.; Yang, Y.H. Naphthoquinones: A continuing source for discovery of therapeutic antineoplastic agents. *Chem. Biol. Drug Des.* **2018**, *91*, 681–690. [CrossRef] [PubMed]
12. Tsai, C.C.; Liu, H.F.; Hsu, K.C.; Yang, J.M.; Chen, C.; Liu, K.K.; Hsu, T.S.; Chao, J.I. 7-Chloro-6-piperidin-1-yl-quinoline-5,8-dione (PT-262), a novel ROCK inhibitor blocks cytoskeleton function and cell migration. *Biochem. Pharmacol.* **2011**, *81*, 856–865. [CrossRef] [PubMed]
13. Daina, A.; Michielin, O.; Zoete, V. SwissADME: A free web tool to evaluate pharmacokinetics, druglikeness and medicinal chemistry friendliness of small molecules. *Sci. Rep.* **2017**, *7*, 42717. [CrossRef] [PubMed]
14. Defant, A.; Guella, G.; Mancini, I. Regioselectivity in the multi-component synthesis of indolizinoquinoline-5,12-dione derivatives. *Eur. J. Org. Chem.* **2006**, 4201–4210. [CrossRef]
15. Silver, R.F.; Holmes, H.L. Synthesis of some 1,6-naphthoquinones and reactions relating to their use in the study of bacterial growth inhibition. *Can. J. Chem.* **1968**, *46*, 1859–1864. [CrossRef]

16. Egleton, J.E.; Thinnes, C.C.; Seden, P.T.; Laurieri, N.; Lee, S.P.; Hadavizadeh, K.S.; Measures, A.R.; Jones, A.M.; Thompson, S.; Varney, A.; et al. Structure–activity relationships and colorimetric properties of specific probes for the putative cancer biomarker human arylamine N-acetyltransferase 1. *Bioorg. Med. Chem.* **2014**, *22*, 3030–3054. [CrossRef] [PubMed]
17. Defant, A.; Rossi, B.; Viliani, G.; Guella, G.; Mancini, I. Metal-assisted regioselectivity in nucleophilic substitutions: A study by Raman spectroscopy and density functional theory calculations. *J. Raman Spectrosc.* **2010**, *41*, 1398–1403. [CrossRef]
18. NCI. Available online: https://dtp.cancer.gov/dtpstandard/cancerscreeningdata/index.jsp (accessed on 30 May 2019).
19. Shaikh, I.A.; Johnson, F.; Grollman, A.P. Streptonigrin.1. Structure-activity relationship among simple bicyclic analogues. Rate dependence of DNA on quinolone reduction potential. *J. Med. Chem.* **1986**, *29*, 1329–1340. [CrossRef] [PubMed]
20. Trott, O.; Olson, A.J. AutoDock Vina: Improving the speed and accuracy of docking with a new scoring function, efficient optimization, and multithreading. *J. Comp. Chem.* **2010**, *31*, 455–461. [CrossRef] [PubMed]
21. Bosco, B.; Defant, A.; Messina, A.; Incitti, T.; Sighel, D.; Bozza, A.; Ciribilli, Y.; Inga, A.; Casarosa, S.; Mancini, I. Synthesis of 2,6-diamino-substituted purine derivatives and evaluation of cell cycle arrest in breast and colorectal cancer cells. *Molecules* **2018**, *23*, 1996. [CrossRef] [PubMed]
22. Systèmes, D. *BIOVIA, Discovery Studio Modeling Environment, Release 2019*; Dassault Systèmes: San Diego, CA, USA, 2019.
23. Swiss ADME. Available online: http://www.swissadme.ch/ (accessed on 28 April 2019).
24. NCI (NIH). Available online: https://dtp.cancer.gov/discovery_development/nci-60/methodology.htm (accessed on 30 May 2019).

Sample Availability: Samples of the compounds **1a–c**, **2a–c** and **3** are available from the authors.

Supplementary Material

Design, synthesis and cancer cell growth inhibition evaluation of new aminoquinone hybrid molecules

Andrea Defant [1] and Ines Mancini [1,*]

[1] Laboratory of Bioorganic Chemistry, Department of Physics, University of Trento, Via Sommarive 14, 38123 Trento, Italy; andrea.defant@unitn.it (A.D.); ines.mancini@unitn.it (I.M.)

*Correspondence: ines.mancini@unitn.it ; Tel.: +39-461-281-548

Table of Contents

Table S1. Energy data (in Kcal/mol) from docking calculation by Autodock Vina for the new ligand molecules **1a**-**1c**, **2a**-**2c** and **3**, in comparison with original and reference ligands.

Molecule	Structure	ΔE *5JCB*[a)]	ΔE 3QX3[b)]	ΔE *2ETK*[c)]
1a	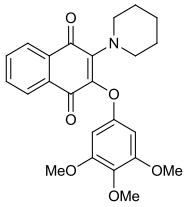	-8.3	-8.7	-8.2
1b	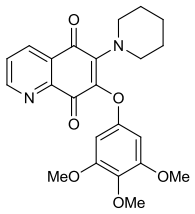	-8.3	-10.4	-7.8
1c	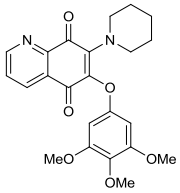	-8.3	-10.2	-8.0
2a	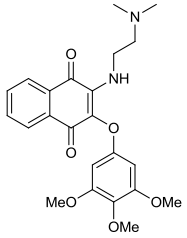	-.8.2	-9.0	-7.6
2b	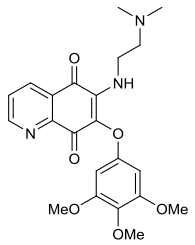	-7.9	-9.4	-6.9
2c	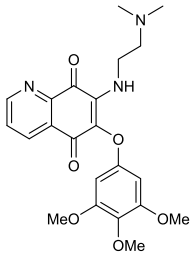	-8.1	-9.6	-6.7
3	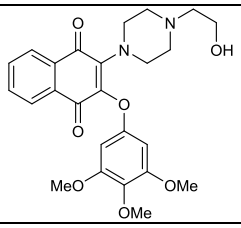	-8.4	-10.6	-7.8

PDB original ligands and reference molecules				
Molecule	**Structure**	**ΔE** *5JCB*[a)]	**ΔE** 3QX3[b)]	**ΔE** *2ETK*[a)]
HFS (original ligand)	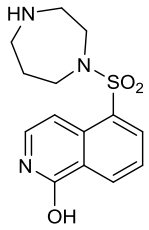	n.d.	n.d.	-8.1
PT-262	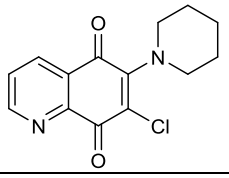	n.d.	n.d.	-7.3
Y-27632	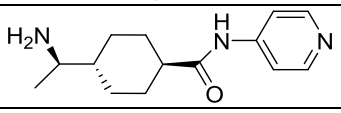	n.d.	n.d.	-6.7
VP-16 (original ligand)	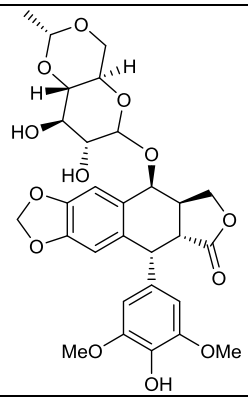	n.d.	-13.3	n.d.
NV4 (original ligand)	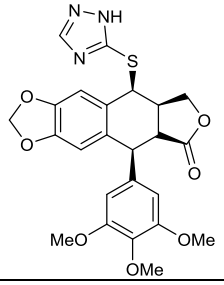	-10.3	n.d.	n.d.
MTP	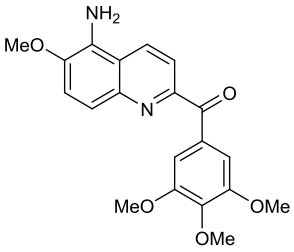	-8.1	n.d.	n.d.

[a)] tubulin (PDB ID: 5JCB),

[b)]human topoisomerase II β (PDB ID: 3QX3)

[c)] human ROCK 1 (PDB ID: 2ETK)

Table S2. ADME Prediction of compounds **1a-c**, **2a-c**, **3** (molecules 1-7, respectively) and reference compounds evaluated by online Server Swiss-ADME.

Molecule 1

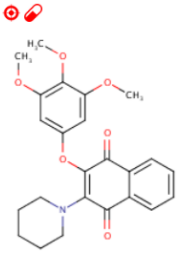

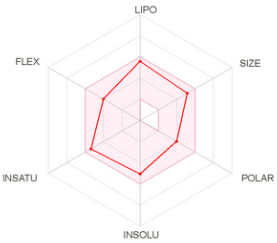

SMILES COc1cc(OC2=C(N3CCCCC3)C(=O)c3c(C2=O)cccc3)cc(c1OC)OC

Physicochemical Properties	
Formula	C24H25NO6
Molecular weight	423.46 g/mol
Num. heavy atoms	31
Num. arom. heavy atoms	12
Fraction Csp3	0.33
Num. rotatable bonds	6
Num. H-bond acceptors	6
Num. H-bond donors	0
Molar Refractivity	118.46
TPSA	74.30 Å²
Lipophilicity	
Log $P_{o/w}$ (iLOGP)	3.43
Log $P_{o/w}$ (XLOGP3)	4.28
Log $P_{o/w}$ (WLOGP)	3.49
Log $P_{o/w}$ (MLOGP)	1.00
Log $P_{o/w}$ (SILICOS-IT)	4.03
Consensus Log $P_{o/w}$	3.25

Water Solubility	
Log *S* (ESOL)	-5.05
Solubility	3.75e-03 mg/ml ; 8.87e-06 mol/l
Class	Moderately soluble
Log *S* (Ali)	-5.55
Solubility	1.19e-03 mg/ml ; 2.80e-06 mol/l
Class	Moderately soluble
Log *S* (SILICOS-IT)	-6.52
Solubility	1.28e-04 mg/ml ; 3.02e-07 mol/l
Class	Poorly soluble
Pharmacokinetics	
GI absorption	High
BBB permeant	Yes
P-gp substrate	No
CYP1A2 inhibitor	No
CYP2C19 inhibitor	Yes
CYP2C9 inhibitor	Yes
CYP2D6 inhibitor	Yes
CYP3A4 inhibitor	Yes
Log K_p (skin permeation)	-5.84 cm/s
Druglikeness	
Lipinski	Yes; 0 violation
Ghose	Yes
Veber	Yes
Egan	Yes
Muegge	Yes
Bioavailability Score	0.56
Medicinal Chemistry	
PAINS	1 alert: quinone_A
Brenk	0 alert
Leadlikeness	No; 2 violations: MW>350, XLOGP3>3.5
Synthetic accessibility	3.92

Molecule 2

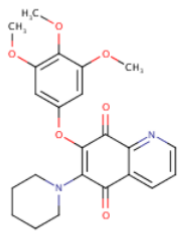

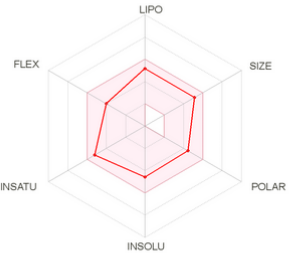

SMILES COc1cc(OC2=C(N3CCCCC3)C(=O)c3c(C2=O)nccc3)cc(c1OC)OC

Physicochemical Properties	
Formula	C23H24N2O6
Molecular weight	424.45 g/mol
Num. heavy atoms	31
Num. arom. heavy atoms	12
Fraction Csp3	0.35
Num. rotatable bonds	6
Num. H-bond acceptors	7
Num. H-bond donors	0
Molar Refractivity	116.26
TPSA	87.19 Å²
Lipophilicity	
Log $P_{o/w}$ (iLOGP)	3.24
Log $P_{o/w}$ (XLOGP3)	3.54
Log $P_{o/w}$ (WLOGP)	2.88
Log $P_{o/w}$ (MLOGP)	0.00
Log $P_{o/w}$ (SILICOS-IT)	3.46
Consensus Log $P_{o/w}$	2.62

Water Solubility	
Log *S* (ESOL)	-4.59
Solubility	1.09e-02 mg/ml ; 2.56e-05 mol/l
Class	Moderately soluble
Log *S* (Ali)	-5.06
Solubility	3.73e-03 mg/ml ; 8.80e-06 mol/l
Class	Moderately soluble
Log *S* (SILICOS-IT)	-6.15
Solubility	3.03e-04 mg/ml ; 7.13e-07 mol/l
Class	Poorly soluble
Pharmacokinetics	
GI absorption	High
BBB permeant	No
P-gp substrate	No
CYP1A2 inhibitor	No
CYP2C19 inhibitor	Yes
CYP2C9 inhibitor	Yes
CYP2D6 inhibitor	No
CYP3A4 inhibitor	Yes
Log K_p (skin permeation)	-6.38 cm/s
Druglikeness	
Lipinski	Yes; 0 violation
Ghose	Yes
Veber	Yes
Egan	Yes
Muegge	Yes
Bioavailability Score	0.56
Medicinal Chemistry	
PAINS	1 alert: quinone_A
Brenk	0 alert
Leadlikeness	No; 2 violations: MW>350, XLOGP3>3.5
Synthetic accessibility	3.85

Molecule 3

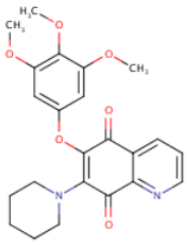

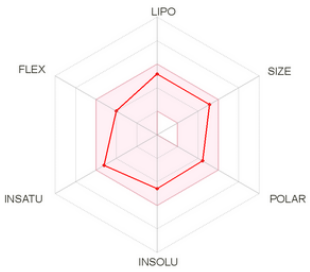

SMILES COc1cc(OC2=C(N3CCCCC3)C(=O)c3c(C2=O)cccn3)cc(c1OC)OC

Physicochemical Properties	
Formula	C23H24N2O6
Molecular weight	424.45 g/mol
Num. heavy atoms	31
Num. arom. heavy atoms	12
Fraction Csp3	0.35
Num. rotatable bonds	6
Num. H-bond acceptors	7
Num. H-bond donors	0
Molar Refractivity	116.26
TPSA	87.19 Å²
Lipophilicity	
Log $P_{o/w}$ (iLOGP)	3.23
Log $P_{o/w}$ (XLOGP3)	3.54
Log $P_{o/w}$ (WLOGP)	2.88
Log $P_{o/w}$ (MLOGP)	0.00
Log $P_{o/w}$ (SILICOS-IT)	3.46
Consensus Log $P_{o/w}$	2.62

Water Solubility	
Log *S* (ESOL)	-4.59
Solubility	1.09e-02 mg/ml ; 2.56e-05 mol/l
Class	Moderately soluble
Log *S* (Ali)	-5.06
Solubility	3.73e-03 mg/ml ; 8.80e-06 mol/l
Class	Moderately soluble
Log *S* (SILICOS-IT)	-6.15
Solubility	3.03e-04 mg/ml ; 7.13e-07 mol/l
Class	Poorly soluble
Pharmacokinetics	
GI absorption	High
BBB permeant	No
P-gp substrate	No
CYP1A2 inhibitor	No
CYP2C19 inhibitor	Yes
CYP2C9 inhibitor	Yes
CYP2D6 inhibitor	No
CYP3A4 inhibitor	Yes
Log K_p (skin permeation)	-6.38 cm/s
Druglikeness	
Lipinski	Yes; 0 violation
Ghose	Yes
Veber	Yes
Egan	Yes
Muegge	Yes
Bioavailability Score	0.56
Medicinal Chemistry	
PAINS	1 alert: quinone_A
Brenk	0 alert
Leadlikeness	No; 2 violations: MW>350, XLOGP3>3.5
Synthetic accessibility	3.82

Molecule 4

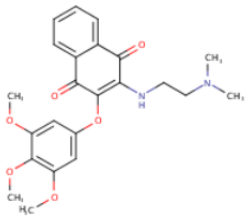

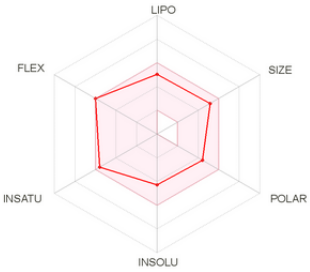

SMILES COc1cc(OC2=C(NCCN(C)C)C(=O)c3c(C2=O)cccc3)cc(c1OC)OC

Physicochemical Properties	
Formula	C23H26N2O6
Molecular weight	426.46 g/mol
Num. heavy atoms	31
Num. arom. heavy atoms	12
Fraction Csp3	0.30
Num. rotatable bonds	9
Num. H-bond acceptors	7
Num. H-bond donors	1
Molar Refractivity	114.66
TPSA	86.33 Å²
Lipophilicity	
Log $P_{o/w}$ (iLOGP)	3.75
Log $P_{o/w}$ (XLOGP3)	3.33
Log $P_{o/w}$ (WLOGP)	2.53
Log $P_{o/w}$ (MLOGP)	0.00
Log $P_{o/w}$ (SILICOS-IT)	3.19
Consensus Log $P_{o/w}$	2.56

Water Solubility	
Log *S* (ESOL)	-4.27
Solubility	2.27e-02 mg/ml ; 5.32e-05 mol/l
Class	Moderately soluble
Log *S* (Ali)	-4.82
Solubility	6.46e-03 mg/ml ; 1.51e-05 mol/l
Class	Moderately soluble
Log *S* (SILICOS-IT)	-6.76
Solubility	7.33e-05 mg/ml ; 1.72e-07 mol/l
Class	Poorly soluble
Pharmacokinetics	
GI absorption	High
BBB permeant	No
P-gp substrate	No
CYP1A2 inhibitor	Yes
CYP2C19 inhibitor	Yes
CYP2C9 inhibitor	Yes
CYP2D6 inhibitor	Yes
CYP3A4 inhibitor	Yes
Log K_p (skin permeation)	-6.54 cm/s
Druglikeness	
Lipinski	Yes; 0 violation
Ghose	Yes
Veber	Yes
Egan	Yes
Muegge	Yes
Bioavailability Score	0.56
Medicinal Chemistry	
PAINS	1 alert: quinone_A
Brenk	0 alert
Leadlikeness	No; 2 violations: MW>350, Rotors>7
Synthetic accessibility	4.02

Molecule 5

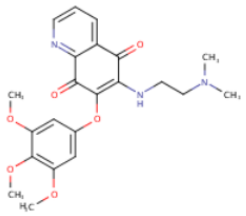

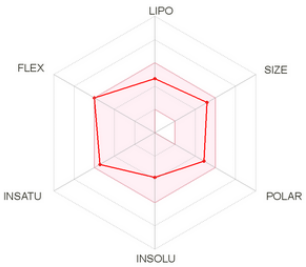

SMILES COc1cc(OC2=C(NCCN(C)C)C(=O)c3c(C2=O)ncccc3)cc(c1OC)OC

Physicochemical Properties	
Formula	C22H25N3O6
Molecular weight	427.45 g/mol
Num. heavy atoms	31
Num. arom. heavy atoms	12
Fraction Csp3	0.32
Num. rotatable bonds	9
Num. H-bond acceptors	8
Num. H-bond donors	1
Molar Refractivity	112.45
TPSA	99.22 Å²
Lipophilicity	
Log $P_{o/w}$ (iLOGP)	3.06
Log $P_{o/w}$ (XLOGP3)	2.60
Log $P_{o/w}$ (WLOGP)	1.93
Log $P_{o/w}$ (MLOGP)	-0.99
Log $P_{o/w}$ (SILICOS-IT)	2.62
Consensus Log $P_{o/w}$	1.84

Water Solubility	
Log *S* (ESOL)	-3.82
Solubility	6.46e-02 mg/ml ; 1.51e-04 mol/l
Class	Soluble
Log *S* (Ali)	-4.33
Solubility	1.99e-02 mg/ml ; 4.65e-05 mol/l
Class	Moderately soluble
Log *S* (SILICOS-IT)	-6.39
Solubility	1.73e-04 mg/ml ; 4.06e-07 mol/l
Class	Poorly soluble
Pharmacokinetics	
GI absorption	High
BBB permeant	No
P-gp substrate	Yes
CYP1A2 inhibitor	Yes
CYP2C19 inhibitor	Yes
CYP2C9 inhibitor	Yes
CYP2D6 inhibitor	No
CYP3A4 inhibitor	Yes
Log K_p (skin permeation)	-7.06 cm/s
Druglikeness	
Lipinski	Yes; 0 violation
Ghose	Yes
Veber	Yes
Egan	Yes
Muegge	Yes
Bioavailability Score	0.56
Medicinal Chemistry	
PAINS	1 alert: quinone_A
Brenk	0 alert
Leadlikeness	No; 2 violations: MW>350, Rotors>7
Synthetic accessibility	3.94

Molecule 6

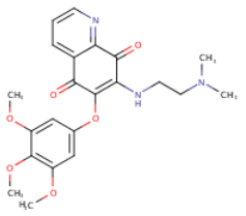

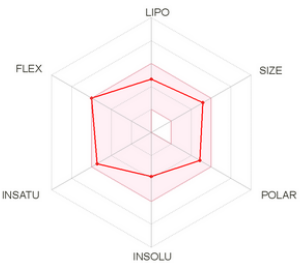

SMILES COc1cc(OC2=C(NCCN(C)C)C(=O)c3c(C2=O)cccn3)cc(c1OC)OC

Physicochemical Properties	
Formula	C22H25N3O6
Molecular weight	427.45 g/mol
Num. heavy atoms	31
Num. arom. heavy atoms	12
Fraction Csp3	0.32
Num. rotatable bonds	9
Num. H-bond acceptors	8
Num. H-bond donors	1
Molar Refractivity	112.45
TPSA	99.22 Å²
Lipophilicity	
Log $P_{o/w}$ (iLOGP)	2.97
Log $P_{o/w}$ (XLOGP3)	2.60
Log $P_{o/w}$ (WLOGP)	1.93
Log $P_{o/w}$ (MLOGP)	-0.99
Log $P_{o/w}$ (SILICOS-IT)	2.62
Consensus Log $P_{o/w}$	1.83

Water Solubility	
Log *S* (ESOL)	-3.82
Solubility	6.46e-02 mg/ml ; 1.51e-04 mol/l
Class	Soluble
Log *S* (Ali)	-4.33
Solubility	1.99e-02 mg/ml ; 4.65e-05 mol/l
Class	Moderately soluble
Log *S* (SILICOS-IT)	-6.39
Solubility	1.73e-04 mg/ml ; 4.06e-07 mol/l
Class	Poorly soluble
Pharmacokinetics	
GI absorption	High
BBB permeant	No
P-gp substrate	Yes
CYP1A2 inhibitor	Yes
CYP2C19 inhibitor	Yes
CYP2C9 inhibitor	Yes
CYP2D6 inhibitor	No
CYP3A4 inhibitor	Yes
Log K_p (skin permeation)	-7.06 cm/s
Druglikeness	
Lipinski	Yes; 0 violation
Ghose	Yes
Veber	Yes
Egan	Yes
Muegge	Yes
Bioavailability Score	0.56
Medicinal Chemistry	
PAINS	1 alert: quinone_A
Brenk	0 alert
Leadlikeness	No; 2 violations: MW>350, Rotors>7
Synthetic accessibility	3.89

Molecule 7

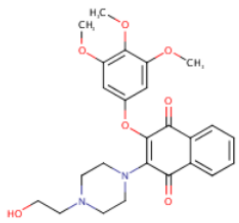

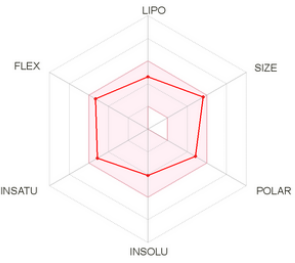

SMILES OCCN1CCN(CC1)C1=C(Oc2cc(OC)c(c(c2)OC)OC)C(=O)c2c(C1=O)cccc2

Physicochemical Properties	
Formula	C25H28N2O7
Molecular weight	468.50 g/mol
Num. heavy atoms	34
Num. arom. heavy atoms	12
Fraction Csp3	0.36
Num. rotatable bonds	8
Num. H-bond acceptors	8
Num. H-bond donors	1
Molar Refractivity	131.24
TPSA	97.77 Å²
Lipophilicity	
Log $P_{o/w}$ (iLOGP)	3.67
Log $P_{o/w}$ (XLOGP3)	2.56
Log $P_{o/w}$ (WLOGP)	1.23
Log $P_{o/w}$ (MLOGP)	-0.36
Log $P_{o/w}$ (SILICOS-IT)	2.82
Consensus Log $P_{o/w}$	1.98

Water Solubility	
Log *S* (ESOL)	-4.09
Solubility	3.80e-02 mg/ml ; 8.12e-05 mol/l
Class	Moderately soluble
Log *S* (Ali)	-4.26
Solubility	2.57e-02 mg/ml ; 5.48e-05 mol/l
Class	Moderately soluble
Log *S* (SILICOS-IT)	-5.77
Solubility	7.99e-04 mg/ml ; 1.71e-06 mol/l
Class	Moderately soluble
Pharmacokinetics	
GI absorption	High
BBB permeant	No
P-gp substrate	Yes
CYP1A2 inhibitor	No
CYP2C19 inhibitor	Yes
CYP2C9 inhibitor	Yes
CYP2D6 inhibitor	No
CYP3A4 inhibitor	Yes
Log K_p (skin permeation)	-7.34 cm/s
Druglikeness	
Lipinski	Yes; 0 violation
Ghose	No; 1 violation: MR>130
Veber	Yes
Egan	Yes
Muegge	Yes
Bioavailability Score	0.56
Medicinal Chemistry	
PAINS	1 alert: quinone_A
Brenk	0 alert
Leadlikeness	No; 2 violations: MW>350, Rotors>7
Synthetic accessibility	4.20

Reference Molecules

Molecule 8

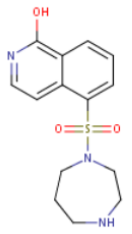

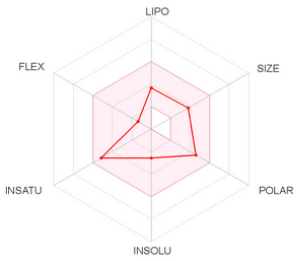

SMILES Oc1nccc2c1cccc2S(=O)(=O)N1CCNCCC1

Physicochemical Properties	
Formula	C14H17N3O3S
Molecular weight	307.37 g/mol
Num. heavy atoms	21
Num. arom. heavy atoms	10
Fraction Csp3	0.36
Num. rotatable bonds	2
Num. H-bond acceptors	6
Num. H-bond donors	2
Molar Refractivity	87.50
TPSA	90.91 Å²
Lipophilicity	
Log $P_{o/w}$ (iLOGP)	1.86
Log $P_{o/w}$ (XLOGP3)	0.93
Log $P_{o/w}$ (WLOGP)	1.24
Log $P_{o/w}$ (MLOGP)	0.55
Log $P_{o/w}$ (SILICOS-IT)	0.59
Consensus Log $P_{o/w}$	1.04

Water Solubility	
Log *S* (ESOL)	-2.55
Solubility	8.62e-01 mg/ml ; 2.81e-03 mol/l
Class	Soluble
Log *S* (Ali)	-2.43
Solubility	1.15e+00 mg/ml ; 3.76e-03 mol/l
Class	Soluble
Log *S* (SILICOS-IT)	-3.81
Solubility	4.73e-02 mg/ml ; 1.54e-04 mol/l
Class	Soluble
Pharmacokinetics	
GI absorption	High
BBB permeant	No
P-gp substrate	Yes
CYP1A2 inhibitor	No
CYP2C19 inhibitor	No
CYP2C9 inhibitor	No
CYP2D6 inhibitor	No
CYP3A4 inhibitor	No
Log K_p (skin permeation)	-7.51 cm/s
Druglikeness	
Lipinski	Yes; 0 violation
Ghose	Yes
Veber	Yes
Egan	Yes
Muegge	Yes
Bioavailability Score	0.55
Medicinal Chemistry	
PAINS	0 alert
Brenk	0 alert
Leadlikeness	Yes
Synthetic accessibility	2.71

Molecule 9

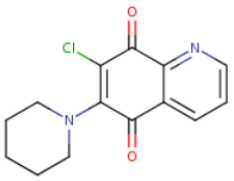

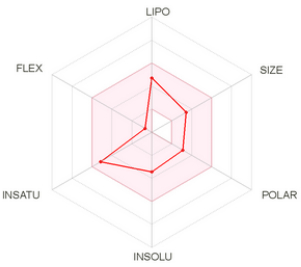

SMILES ClC1=C(N2CCCCC2)C(=O)c2c(C1=O)nccc2

Physicochemical Properties	
Formula	C14H13ClN2O2
Molecular weight	276.72 g/mol
Num. heavy atoms	19
Num. arom. heavy atoms	6
Fraction Csp3	0.36
Num. rotatable bonds	1
Num. H-bond acceptors	3
Num. H-bond donors	0
Molar Refractivity	75.57
TPSA	50.27 Å²

Lipophilicity	
Log $P_{o/w}$ (iLOGP)	1.88
Log $P_{o/w}$ (XLOGP3)	2.73
Log $P_{o/w}$ (WLOGP)	2.02
Log $P_{o/w}$ (MLOGP)	0.55
Log $P_{o/w}$ (SILICOS-IT)	2.88
Consensus Log $P_{o/w}$	2.01

Water Solubility	
Log *S* (ESOL)	-3.44
Solubility	9.97e-02 mg/ml ; 3.60e-04 mol/l
Class	Soluble
Log *S* (Ali)	-3.44
Solubility	1.01e-01 mg/ml ; 3.63e-04 mol/l
Class	Soluble
Log *S* (SILICOS-IT)	-4.22
Solubility	1.66e-02 mg/ml ; 6.01e-05 mol/l
Class	Moderately soluble

Pharmacokinetics	
GI absorption	High
BBB permeant	Yes
P-gp substrate	No
CYP1A2 inhibitor	Yes
CYP2C19 inhibitor	Yes
CYP2C9 inhibitor	No
CYP2D6 inhibitor	No
CYP3A4 inhibitor	Yes
Log K_p (skin permeation)	-6.05 cm/s

Druglikeness	
Lipinski	Yes; 0 violation
Ghose	Yes
Veber	Yes
Egan	Yes
Muegge	Yes
Bioavailability Score	0.55

Medicinal Chemistry	
PAINS	2 alerts: ene_one_hal, quinone_A
Brenk	0 alert
Leadlikeness	Yes
Synthetic accessibility	2.94

Molecule 10

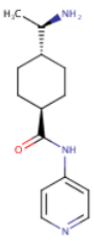

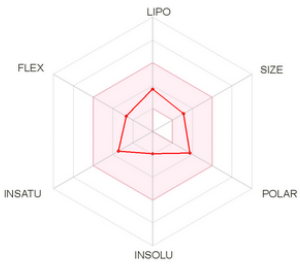

SMILES C[C@H]([C@@H]1CC[C@H](CC1)C(=O)Nc1ccncc1)N

Physicochemical Properties	
Formula	C14H21N3O
Molecular weight	247.34 g/mol
Num. heavy atoms	18
Num. arom. heavy atoms	6
Fraction Csp3	0.57
Num. rotatable bonds	4
Num. H-bond acceptors	3
Num. H-bond donors	2
Molar Refractivity	72.79
TPSA	68.01 Å²

Lipophilicity	
Log $P_{o/w}$ (iLOGP)	2.20
Log $P_{o/w}$ (XLOGP3)	0.95
Log $P_{o/w}$ (WLOGP)	1.98
Log $P_{o/w}$ (MLOGP)	1.13
Log $P_{o/w}$ (SILICOS-IT)	1.56
Consensus Log $P_{o/w}$	1.57

Water Solubility	
Log *S* (ESOL)	-1.95
Solubility	2.75e+00 mg/ml ; 1.11e-02 mol/l
Class	Very soluble
Log *S* (Ali)	-1.97
Solubility	2.68e+00 mg/ml ; 1.08e-02 mol/l
Class	Very soluble
Log *S* (SILICOS-IT)	-3.31
Solubility	1.20e-01 mg/ml ; 4.85e-04 mol/l
Class	Soluble

Pharmacokinetics	
GI absorption	High
BBB permeant	Yes
P-gp substrate	No
CYP1A2 inhibitor	No
CYP2C19 inhibitor	No
CYP2C9 inhibitor	No
CYP2D6 inhibitor	No
CYP3A4 inhibitor	No
Log K_p (skin permeation)	-7.13 cm/s

Druglikeness	
Lipinski	Yes; 0 violation
Ghose	Yes
Veber	Yes
Egan	Yes
Muegge	Yes
Bioavailability Score	0.55

Medicinal Chemistry	
PAINS	0 alert
Brenk	0 alert
Leadlikeness	No; 1 violation: MW<250
Synthetic accessibility	2.73

Molecule 11

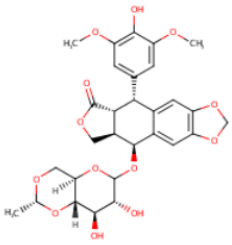

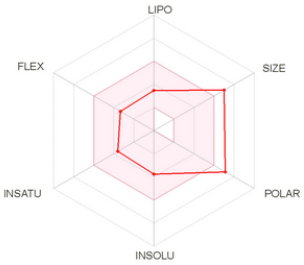

SMILES COc1cc(cc(c1O)OC)[C@H]1[C@H]2C(=O)OC[C@@H]2[C@@H](c2c1cc1OCOc1c2)OC1O[C@@H]2CO[C@H](O[C@H]2[C@@H]([C@H]1O)O)C

Physicochemical Properties	
Formula	C29H32O13
Molecular weight	588.56 g/mol
Num. heavy atoms	42
Num. arom. heavy atoms	12
Fraction Csp3	0.55
Num. rotatable bonds	5
Num. H-bond acceptors	13
Num. H-bond donors	3
Molar Refractivity	139.11
TPSA	160.83 Å²
Lipophilicity	
Log $P_{o/w}$ (iLOGP)	3.24
Log $P_{o/w}$ (XLOGP3)	0.60
Log $P_{o/w}$ (WLOGP)	1.01
Log $P_{o/w}$ (MLOGP)	-0.14
Log $P_{o/w}$ (SILICOS-IT)	0.95
Consensus Log $P_{o/w}$	1.13

Water Solubility	
Log *S* (ESOL)	-3.75
Solubility	1.05e-01 mg/ml ; 1.78e-04 mol/l
Class	Soluble
Log *S* (Ali)	-3.55
Solubility	1.65e-01 mg/ml ; 2.81e-04 mol/l
Class	Soluble
Log *S* (SILICOS-IT)	-3.18
Solubility	3.85e-01 mg/ml ; 6.55e-04 mol/l
Class	Soluble
Pharmacokinetics	
GI absorption	Low
BBB permeant	No
P-gp substrate	Yes
CYP1A2 inhibitor	No
CYP2C19 inhibitor	No
CYP2C9 inhibitor	No
CYP2D6 inhibitor	Yes
CYP3A4 inhibitor	No
Log K_p (skin permeation)	-9.46 cm/s
Druglikeness	
Lipinski	No; 2 violations: MW>500, NorO>10
Ghose	No; 3 violations: MW>480, MR>130, #atoms>70
Veber	No; 1 violation: TPSA>140
Egan	No; 1 violation: TPSA>131.6
Muegge	No; 2 violations: TPSA>150, H-acc>10
Bioavailability Score	0.17
Medicinal Chemistry	
PAINS	0 alert
Brenk	0 alert
Leadlikeness	No; 1 violation: MW>350
Synthetic accessibility	6.27

Molecule 12

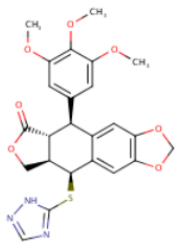

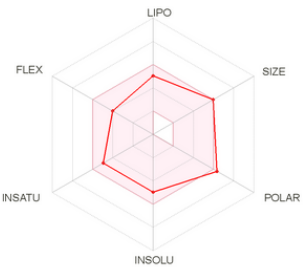

SMILES COc1c(OC)cc(cc1OC)[C@@H]1[C@H]2C(=O)OC[C@@H]2[C@@H](c2c1cc1OCOc1c2)Sc1[nH]ncn1

Physicochemical Properties	
Formula	C24H23N3O7S
Molecular weight	497.52 g/mol
Num. heavy atoms	35
Num. arom. heavy atoms	17
Fraction Csp3	0.38
Num. rotatable bonds	6
Num. H-bond acceptors	9
Num. H-bond donors	1
Molar Refractivity	123.87
TPSA	139.32 Å²
Lipophilicity	
Log $P_{o/w}$ (iLOGP)	2.78
Log $P_{o/w}$ (XLOGP3)	3.30
Log $P_{o/w}$ (WLOGP)	3.00
Log $P_{o/w}$ (MLOGP)	1.60
Log $P_{o/w}$ (SILICOS-IT)	3.41
Consensus Log $P_{o/w}$	2.82

Water Solubility	
Log *S* (ESOL)	-4.97
Solubility	5.37e-03 mg/ml ; 1.08e-05 mol/l
Class	Moderately soluble
Log *S* (Ali)	-5.90
Solubility	6.24e-04 mg/ml ; 1.26e-06 mol/l
Class	Moderately soluble
Log *S* (SILICOS-IT)	-6.34
Solubility	2.30e-04 mg/ml ; 4.61e-07 mol/l
Class	Poorly soluble
Pharmacokinetics	
GI absorption	Low
BBB permeant	No
P-gp substrate	No
CYP1A2 inhibitor	No
CYP2C19 inhibitor	No
CYP2C9 inhibitor	Yes
CYP2D6 inhibitor	Yes
CYP3A4 inhibitor	Yes
Log K_p (skin permeation)	-6.99 cm/s
Druglikeness	
Lipinski	Yes; 0 violation
Ghose	No; 1 violation: MW>480
Veber	Yes
Egan	No; 1 violation: TPSA>131.6
Muegge	Yes
Bioavailability Score	0.55
Medicinal Chemistry	
PAINS	0 alert
Brenk	0 alert
Leadlikeness	No; 1 violation: MW>350
Synthetic accessibility	5.13

Molecule 13

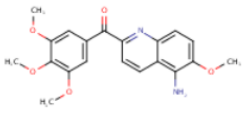

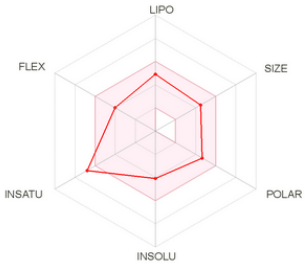

SMILES COc1cc(cc(c1OC)OC)C(=O)c1ccc2c(n1)ccc(c2N)OC

Physicochemical Properties	
Formula	C20H20N2O5
Molecular weight	368.38 g/mol
Num. heavy atoms	27
Num. arom. heavy atoms	16
Fraction Csp3	0.20
Num. rotatable bonds	6
Num. H-bond acceptors	6
Num. H-bond donors	1
Molar Refractivity	101.99
TPSA	92.90 Å²

Lipophilicity	
Log $P_{o/w}$ (iLOGP)	3.22
Log $P_{o/w}$ (XLOGP3)	3.07
Log $P_{o/w}$ (WLOGP)	3.09
Log $P_{o/w}$ (MLOGP)	0.63
Log $P_{o/w}$ (SILICOS-IT)	3.35
Consensus Log $P_{o/w}$	2.67

Water Solubility	
Log *S* (ESOL)	-4.10
Solubility	2.92e-02 mg/ml ; 7.93e-05 mol/l
Class	Moderately soluble
Log *S* (Ali)	-4.69
Solubility	7.56e-03 mg/ml ; 2.05e-05 mol/l
Class	Moderately soluble
Log *S* (SILICOS-IT)	-6.27
Solubility	2.00e-04 mg/ml ; 5.42e-07 mol/l
Class	Poorly soluble

Pharmacokinetics	
GI absorption	High
BBB permeant	No
P-gp substrate	No
CYP1A2 inhibitor	Yes
CYP2C19 inhibitor	Yes
CYP2C9 inhibitor	Yes
CYP2D6 inhibitor	Yes
CYP3A4 inhibitor	Yes
Log K_p (skin permeation)	-6.37 cm/s

Druglikeness	
Lipinski	Yes; 0 violation
Ghose	Yes
Veber	Yes
Egan	Yes
Muegge	Yes
Bioavailability Score	0.55

Medicinal Chemistry	
PAINS	0 alert
Brenk	1 alert: aniline
Leadlikeness	No; 1 violation: MW>350
Synthetic accessibility	2.83

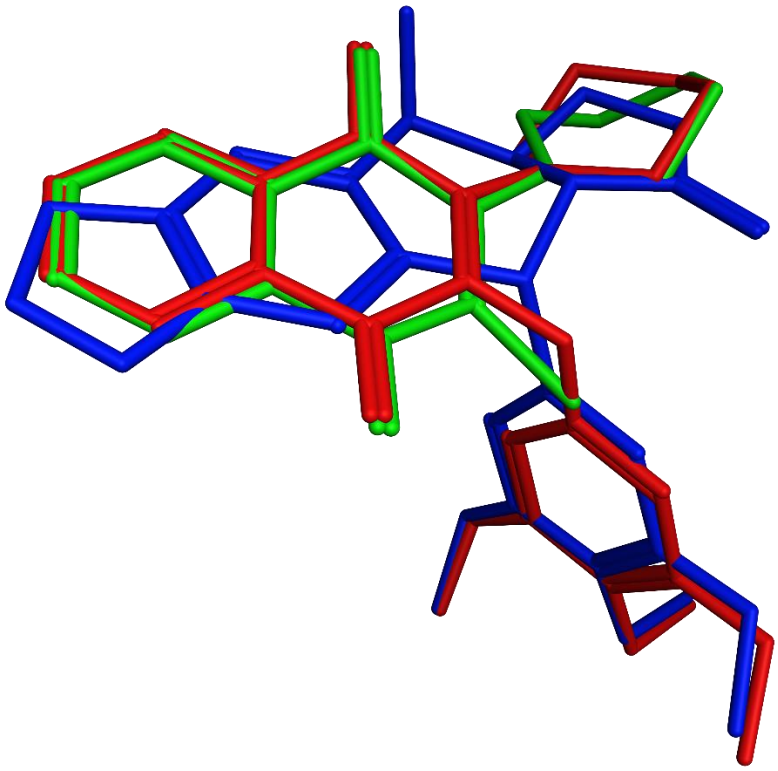

Figure S1. Overlapping of the energy minimized structures **1b** (in red), PT-262 (in green) and podophyllotoxin (in blue). Hydrogen atoms are omitted for clarity.

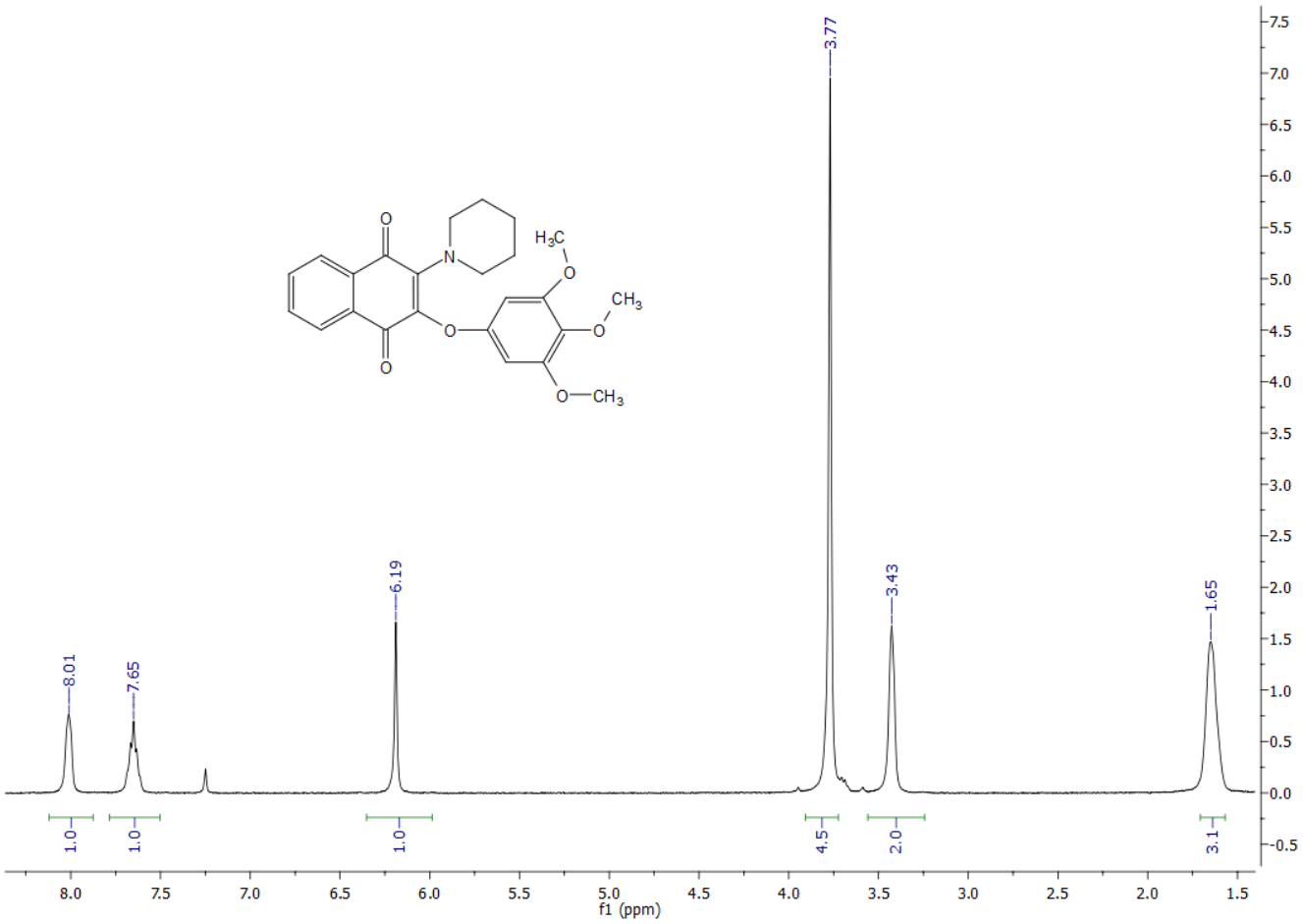

Figure S2. ^{1}HNMR spectrum (400MHz, $CDCl_3$) of compound **1a.**

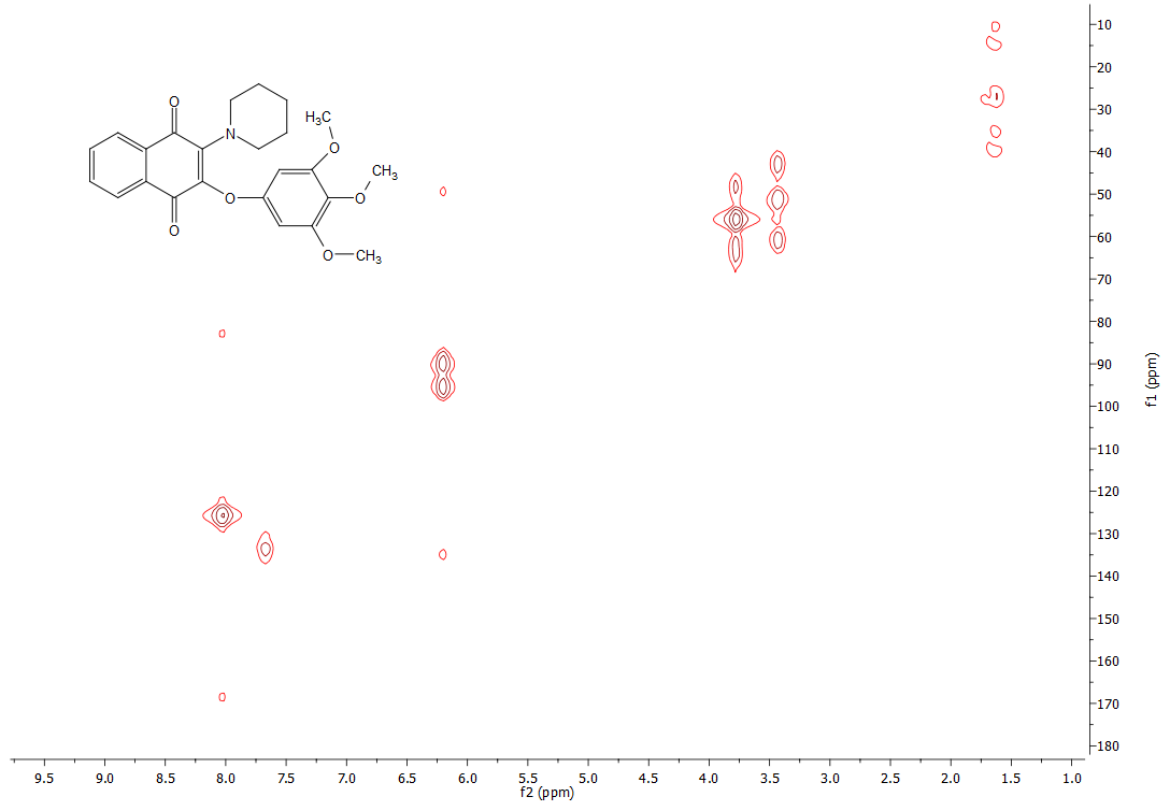

Figure S3. $^{1}H,^{13}C$ correlations by HSQC experiment (400MHz, $CDCl_3$) of **1a.**

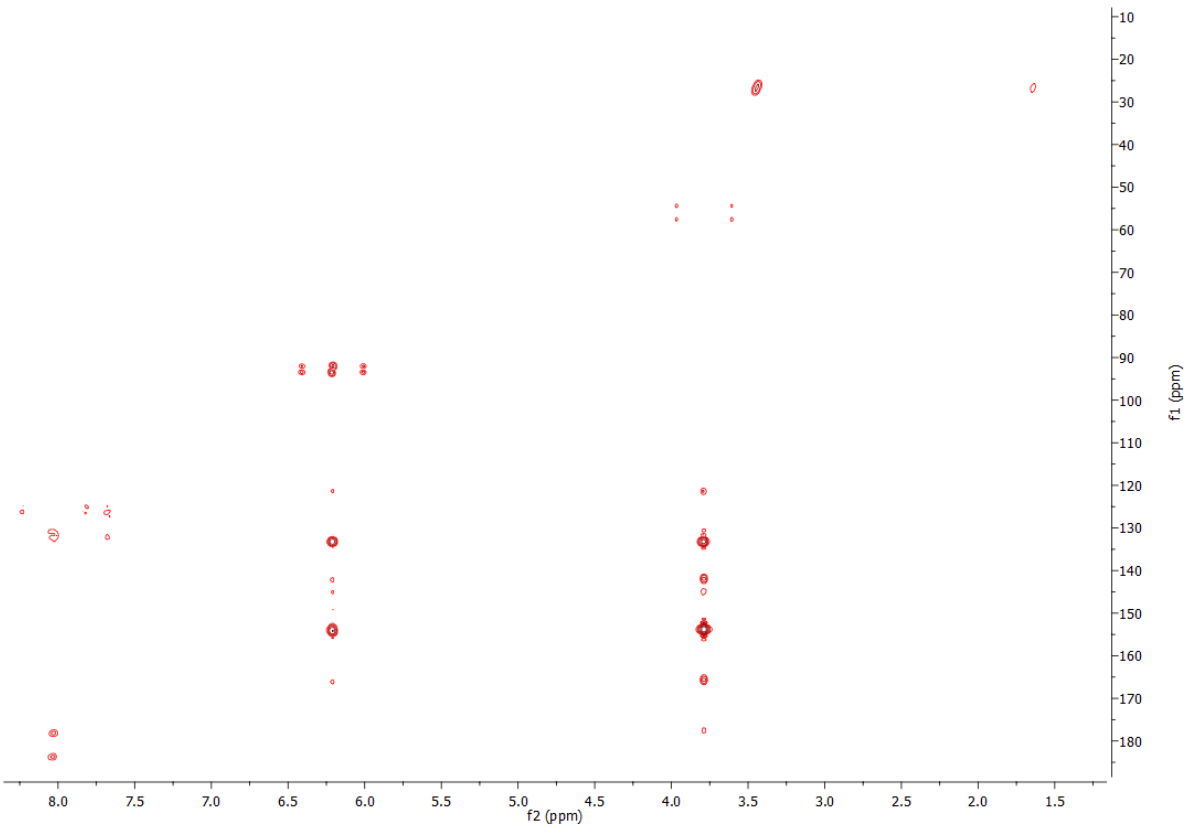

Figure S4. $^{1}H,^{13}C$ long range correlations by HMBC experiment (400MHz, $CDCl_3$) of **1a.**

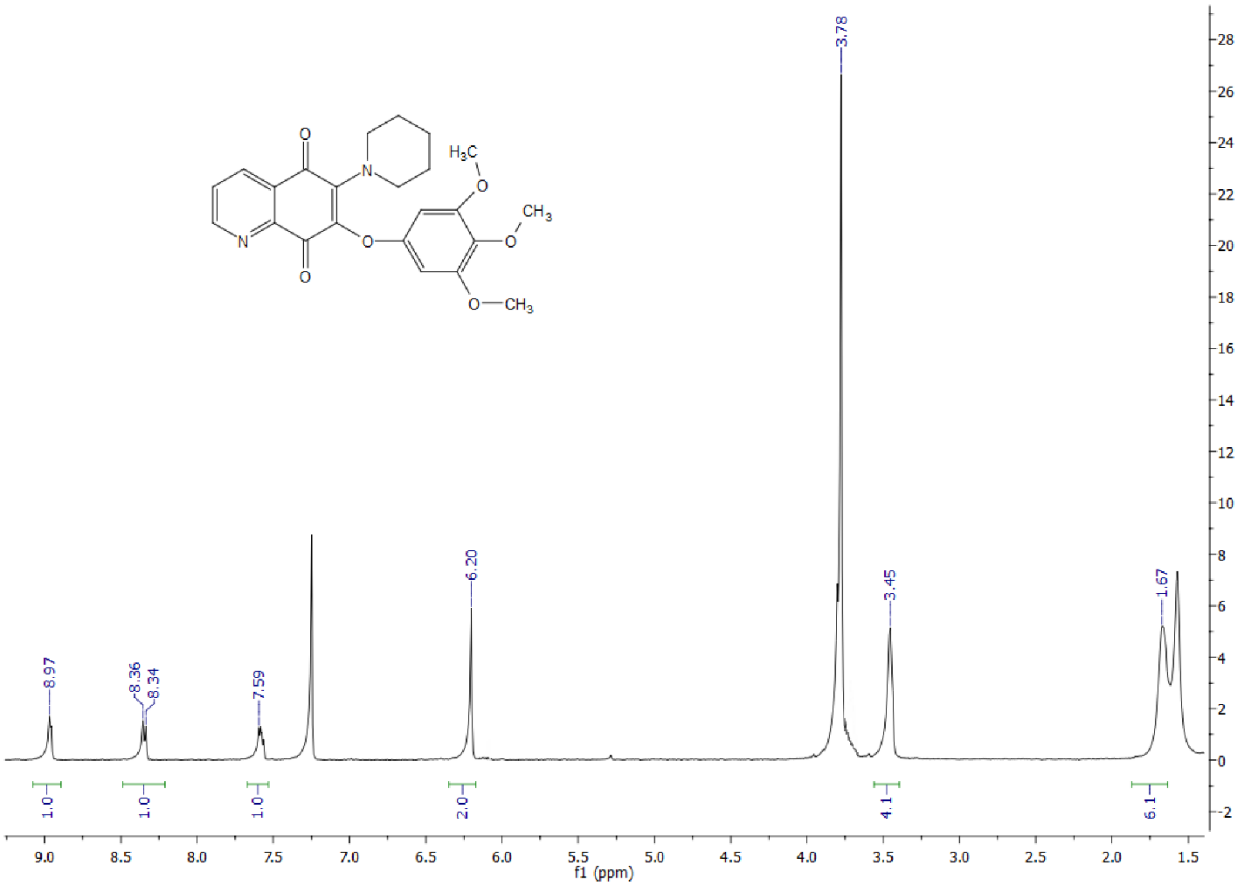

Figure S5. ^{1}HNMR spectrum (400MHz, $CDCl_3$) of compound **1b.**

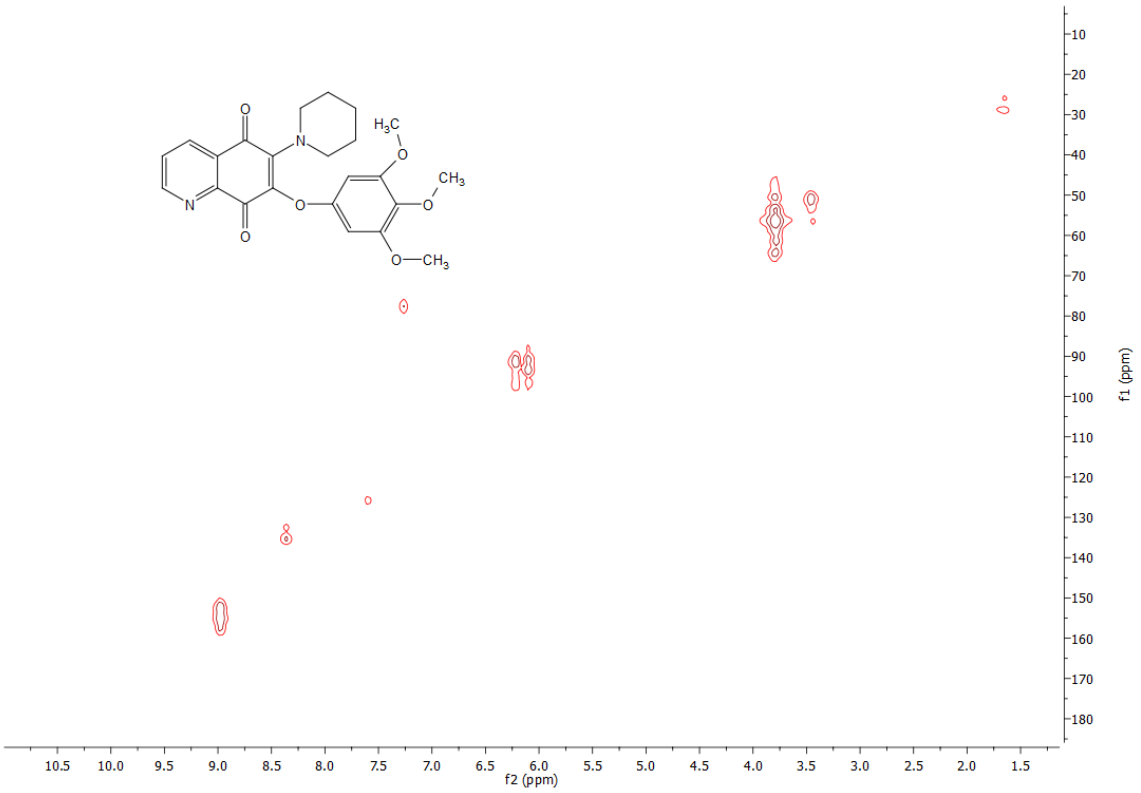

Figure S6. $^{1}H,^{13}C$ correlations by HSQC experiment (400MHz, $CDCl_3$) of **1b.**

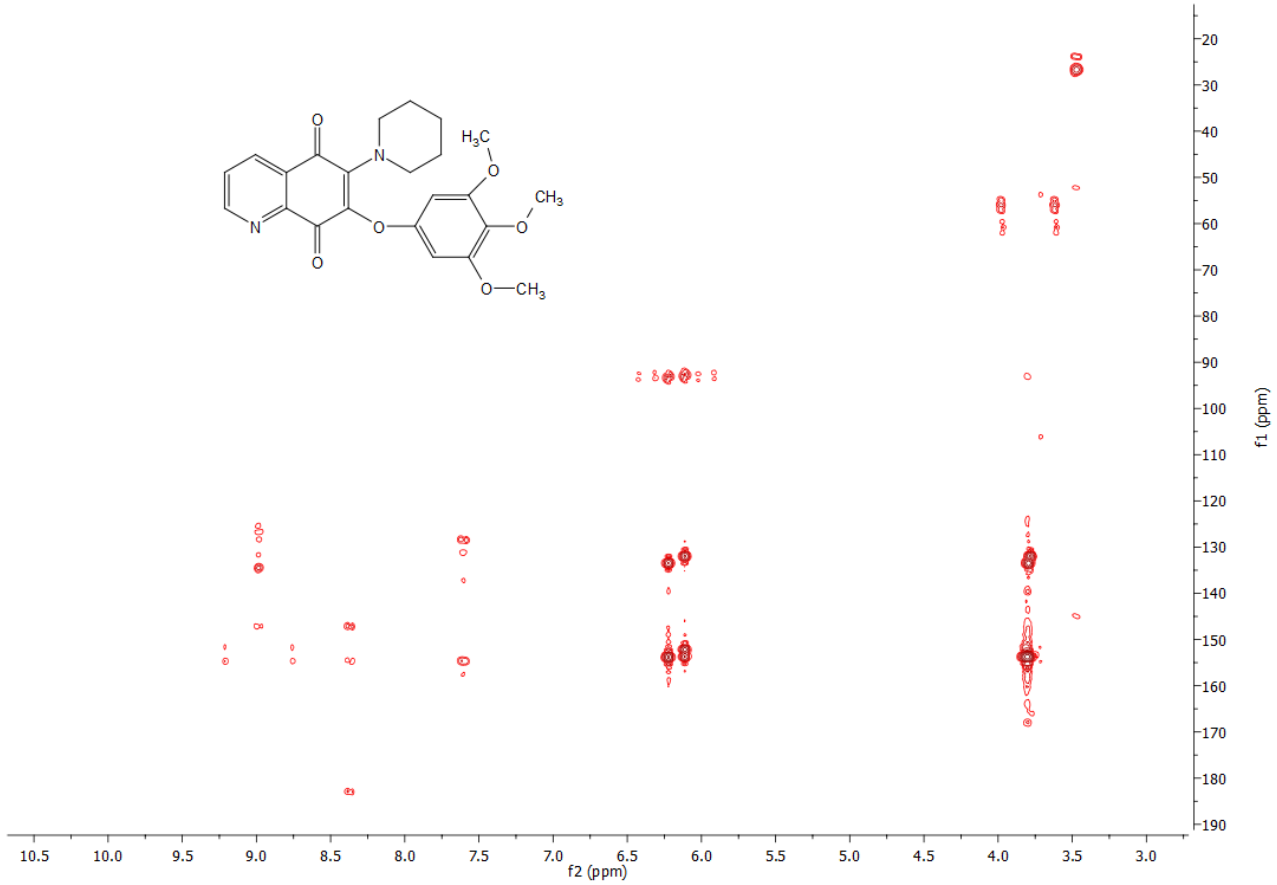

Figure S7. $^{1}H,^{13}C$ long range correlations by HMBC experiment (400MHz, $CDCl_3$) of **1b.**

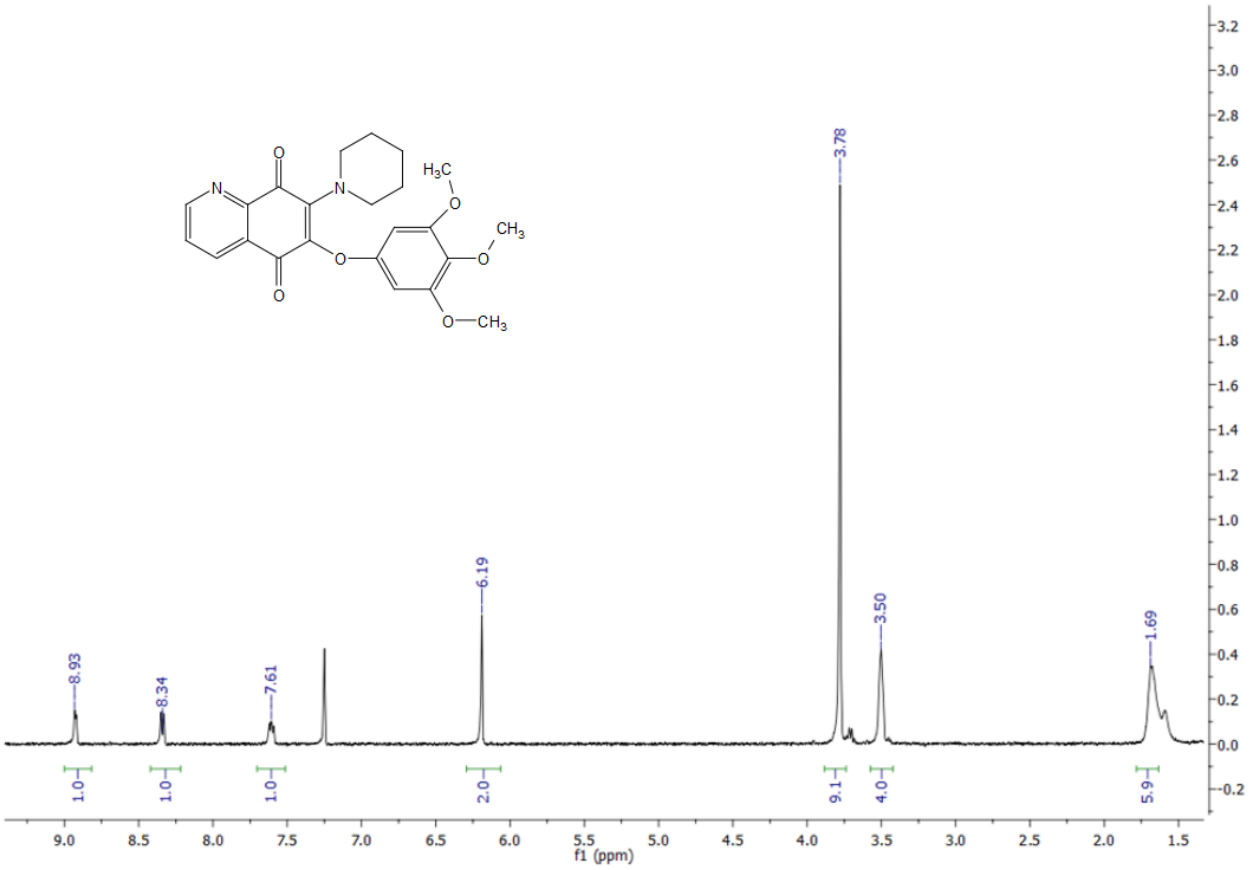

Figure S8. ^{1}HNMR spectrum (400MHz, $CDCl_3$) of compound **1c.**

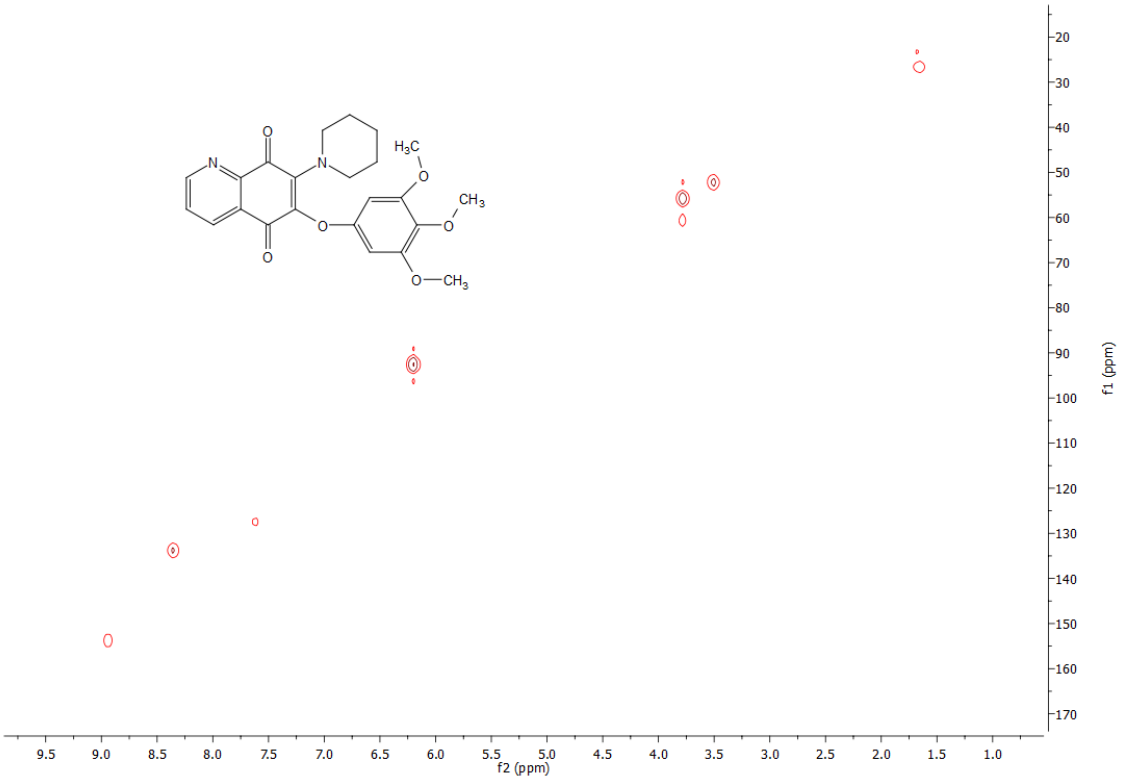

Figure S9. $^{1}H,^{13}C$ correlations by HSQC experiment (400MHz, $CDCl_3$) of **1c.**

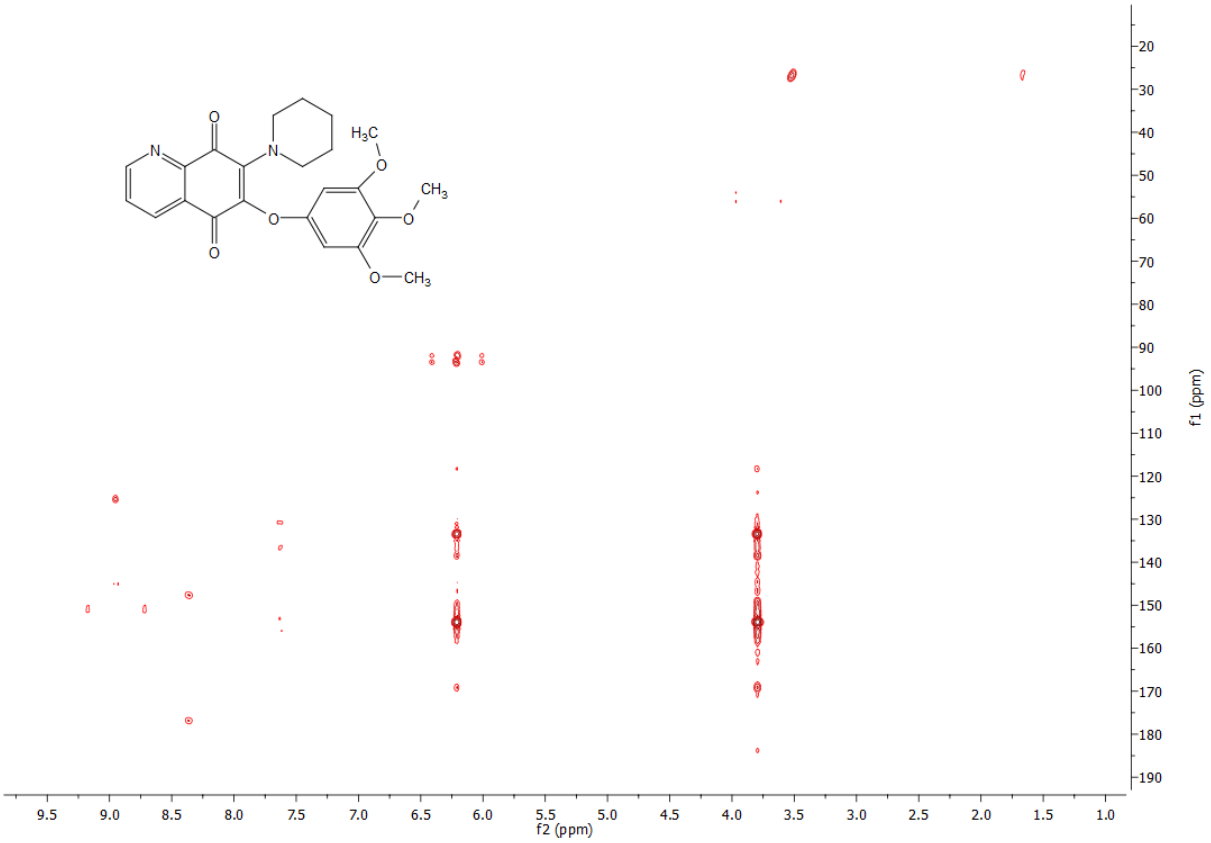

Figure S10. $^{1}H,^{13}C$ long range correlations by HMBC experiment (400MHz, $CDCl_3$) of **1c.**

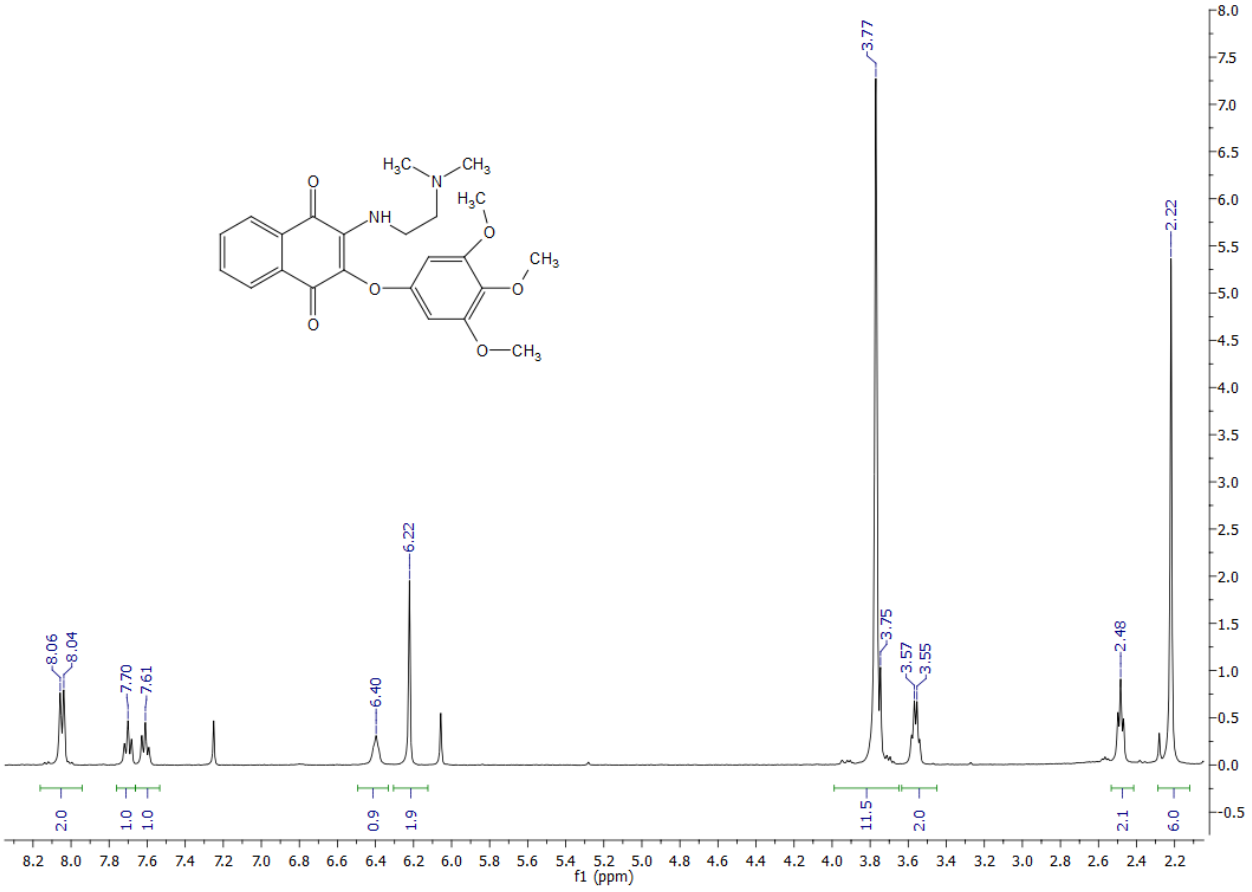

Figure S11. [1]HNMR spectrum (400MHz, $CDCl_3$) of compound **2a.**

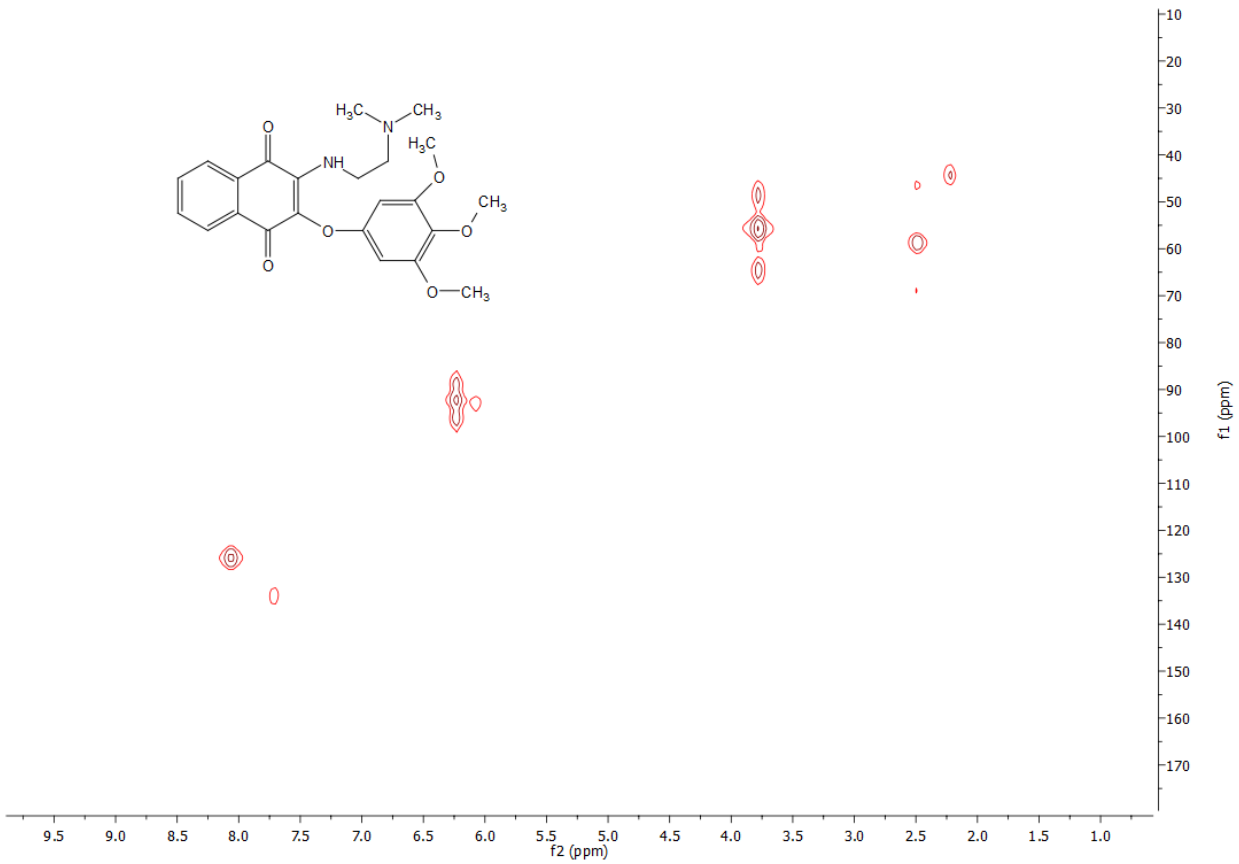

Figure S12. $^{1}H,^{13}C$ correlations by HSQC experiment (400MHz, $CDCl_3$) of **2a.**

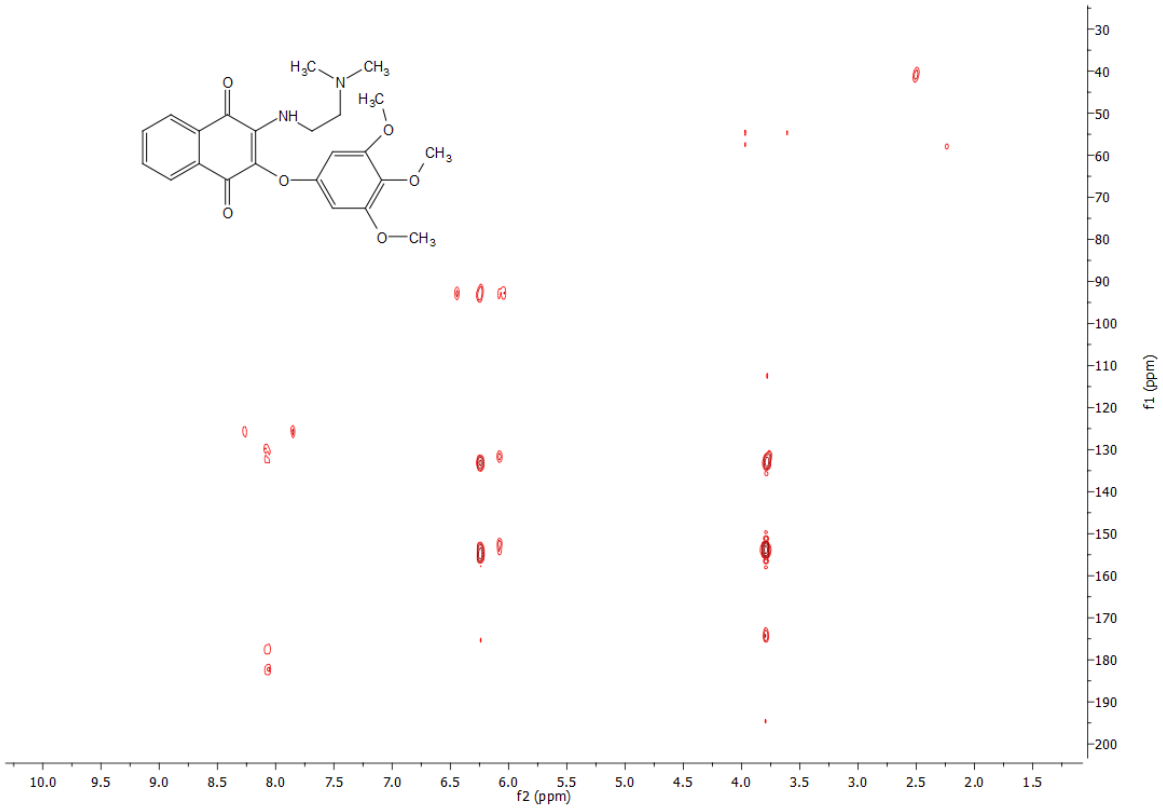

Figure S13. $^{1}H,^{13}C$ long range correlations by HMBC experiment (400MHz, $CDCl_3$) of **2a.**

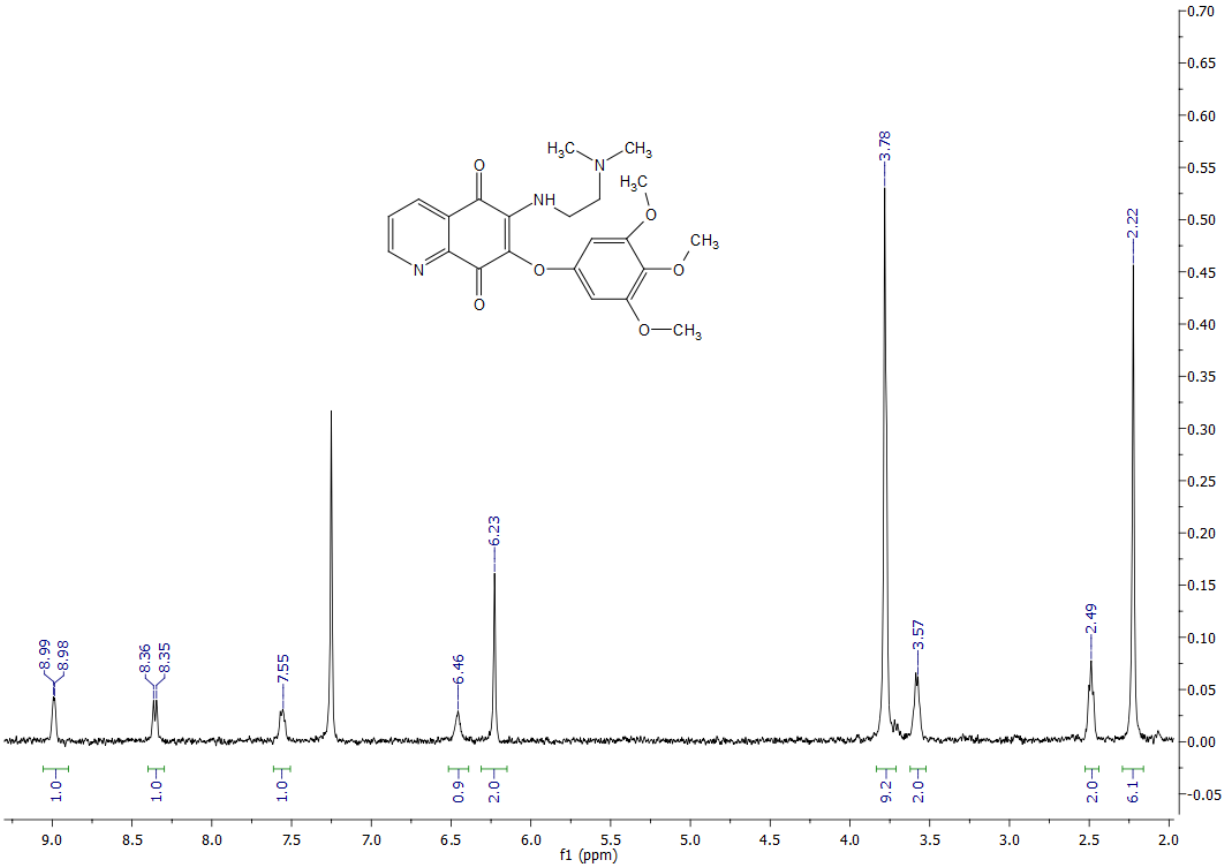

Figure S14. ^{1}HNMR spectrum (400MHz, $CDCl_3$) of compound **2b.**

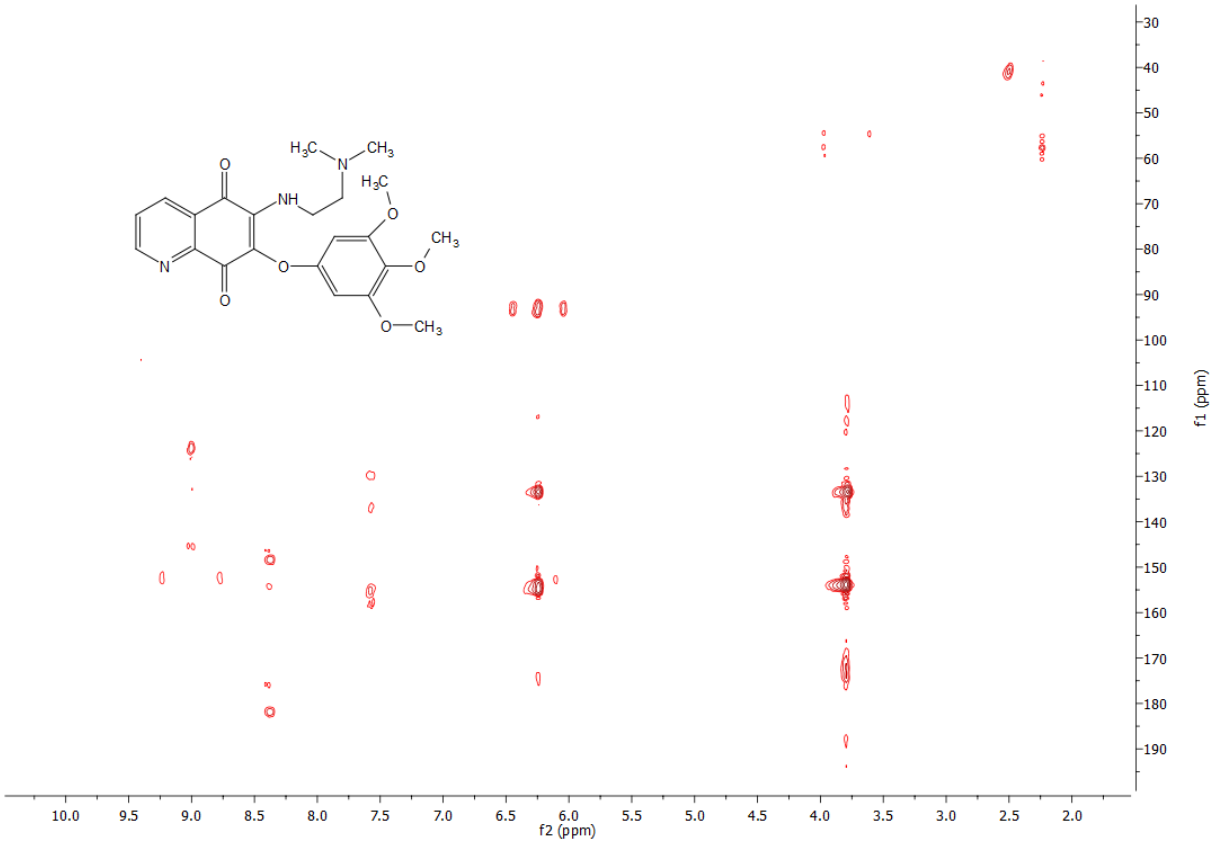

Figure S15. ^{1}H,^{13}C long range correlations by HMBC experiment (400MHz, $CDCl_3$) of **2b.**

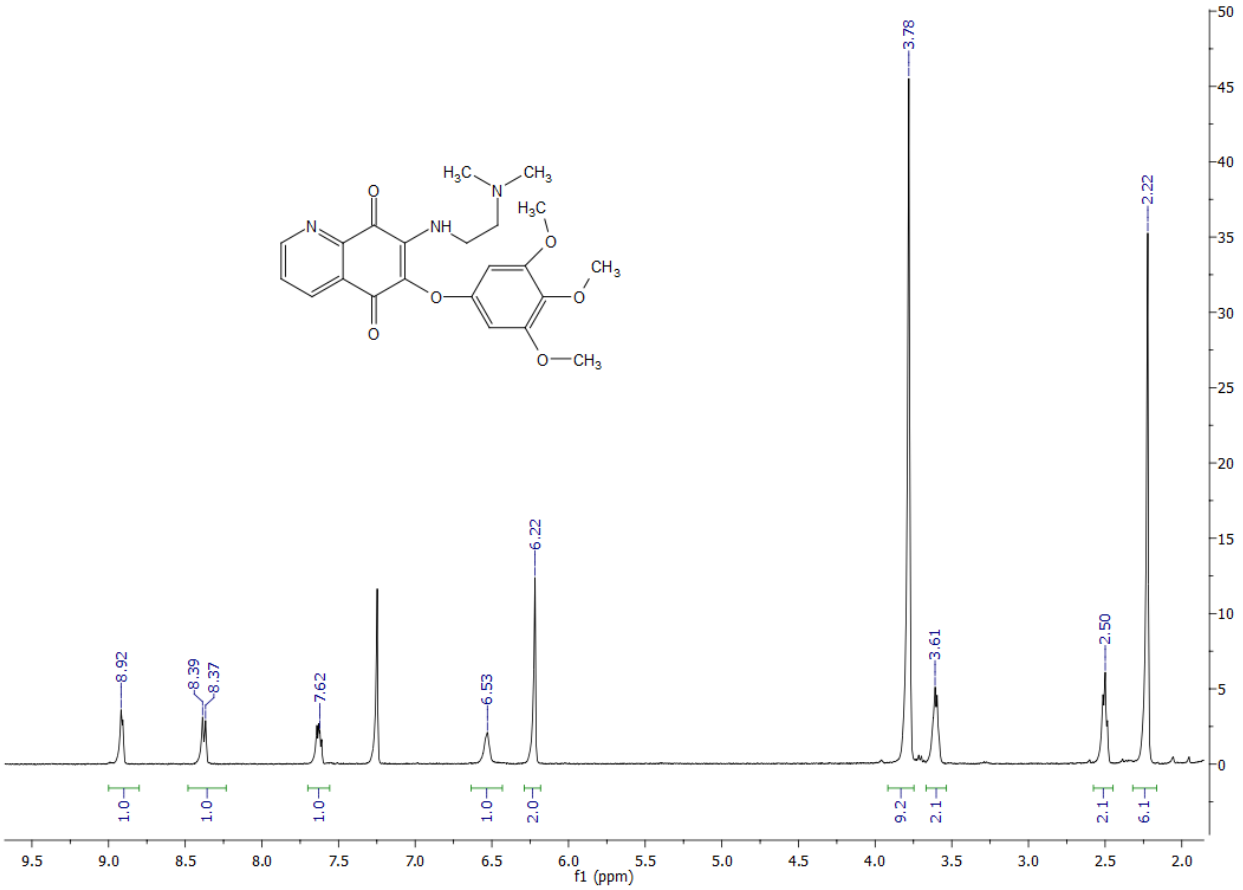

Figure S16. [1]HNMR spectrum (400MHz, $CDCl_3$) of compound **2c.**

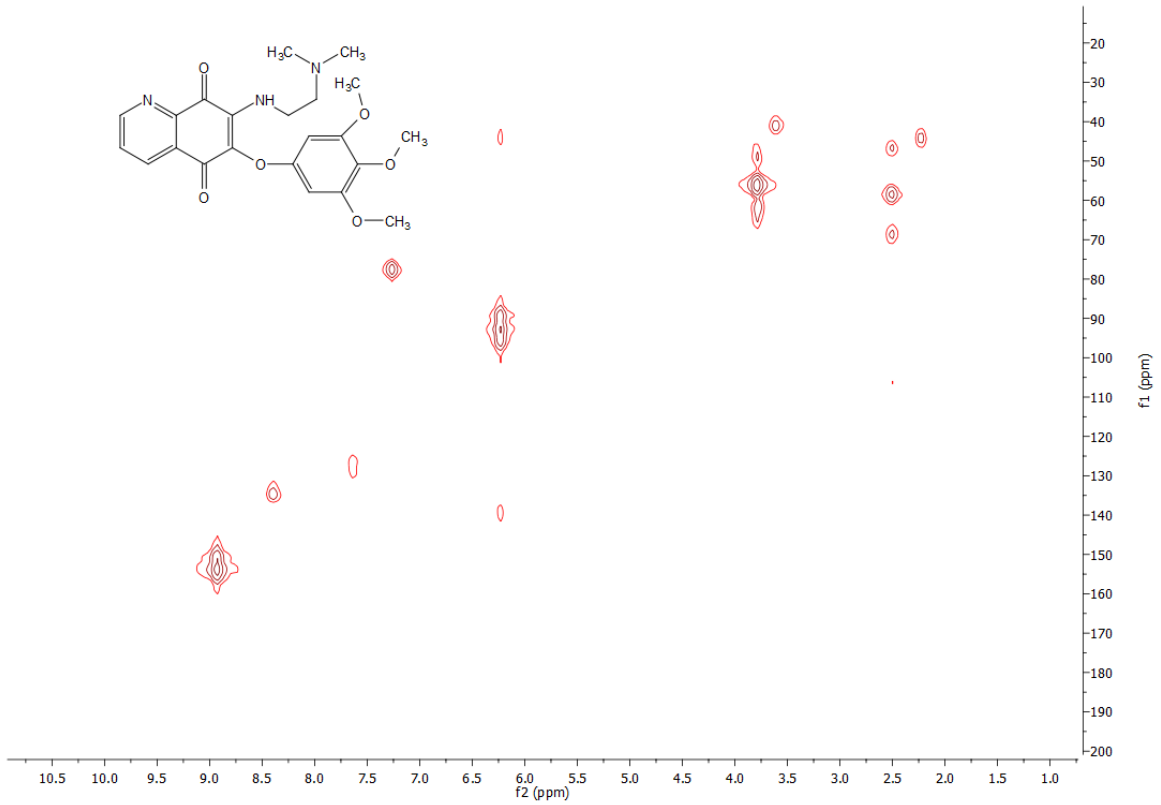

Figure S17. $^{1}H,^{13}C$ correlations by HSQC experiment (400MHz, $CDCl_3$) of **2c.**

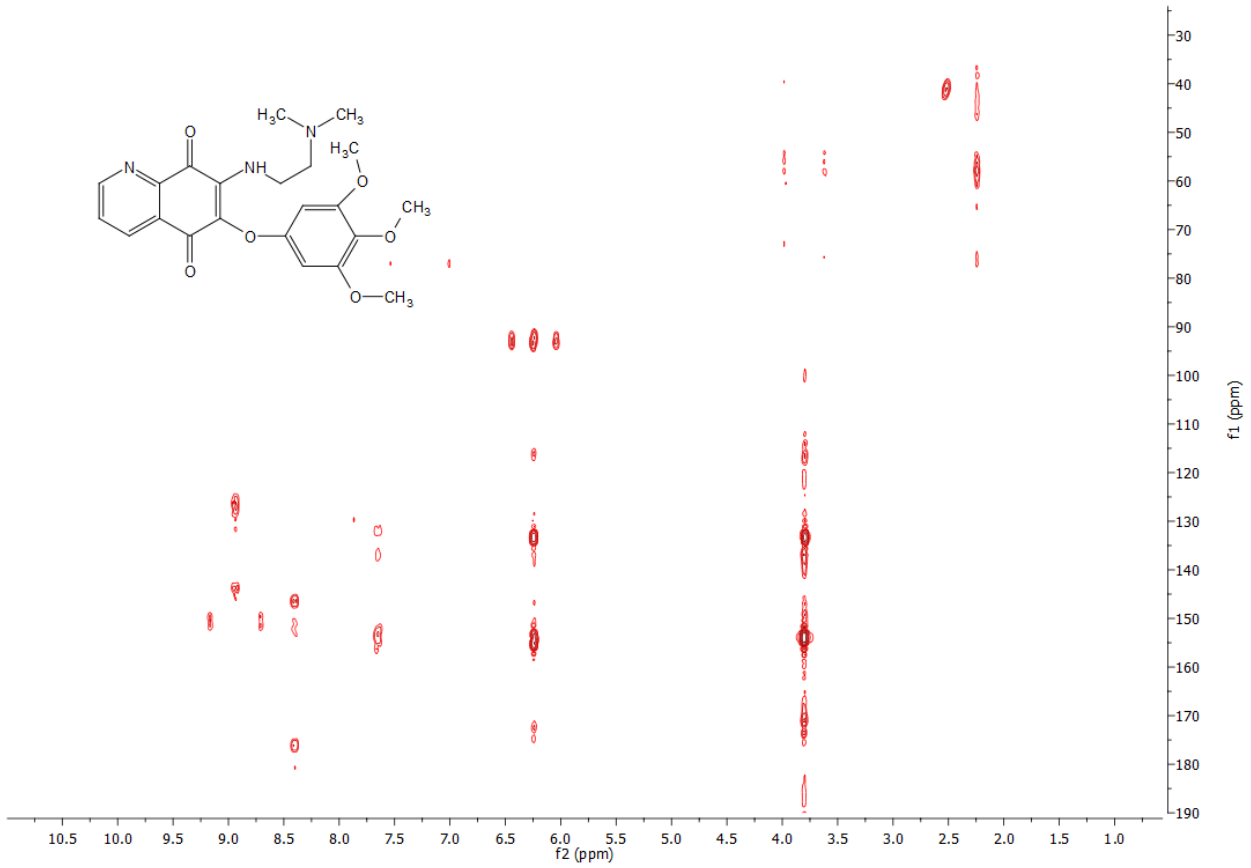

Figure S18. $^{1}H,^{13}C$ long range correlations by HMBC experiment (400MHz, $CDCl_3$) of **2c.**

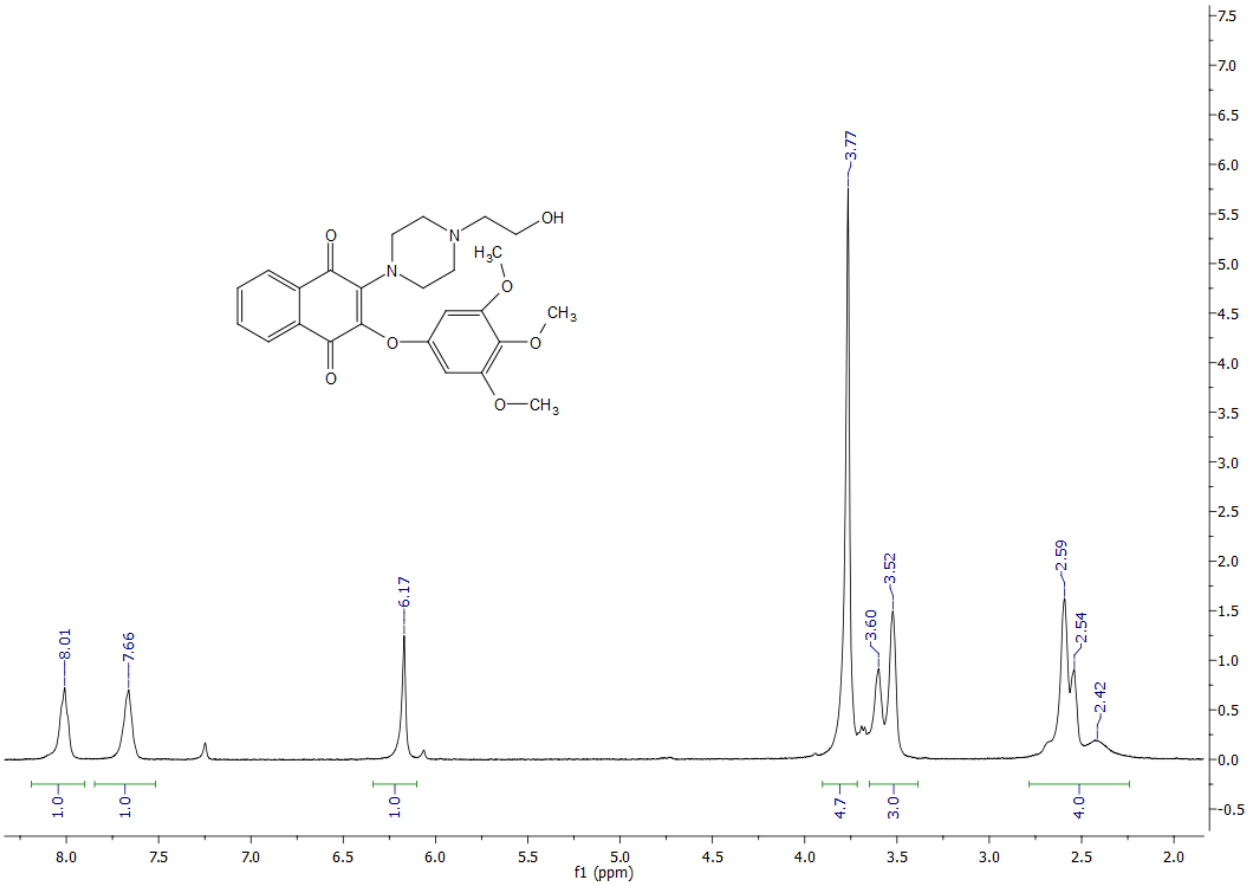

Figure S19. ^{1}HNMR spectrum (400MHz, $CDCl_3$) of compound **3.**

Figure S20. $^{1}H,^{13}C$ correlations by HSQC experiment (400MHz, $CDCl_3$) of **3.**

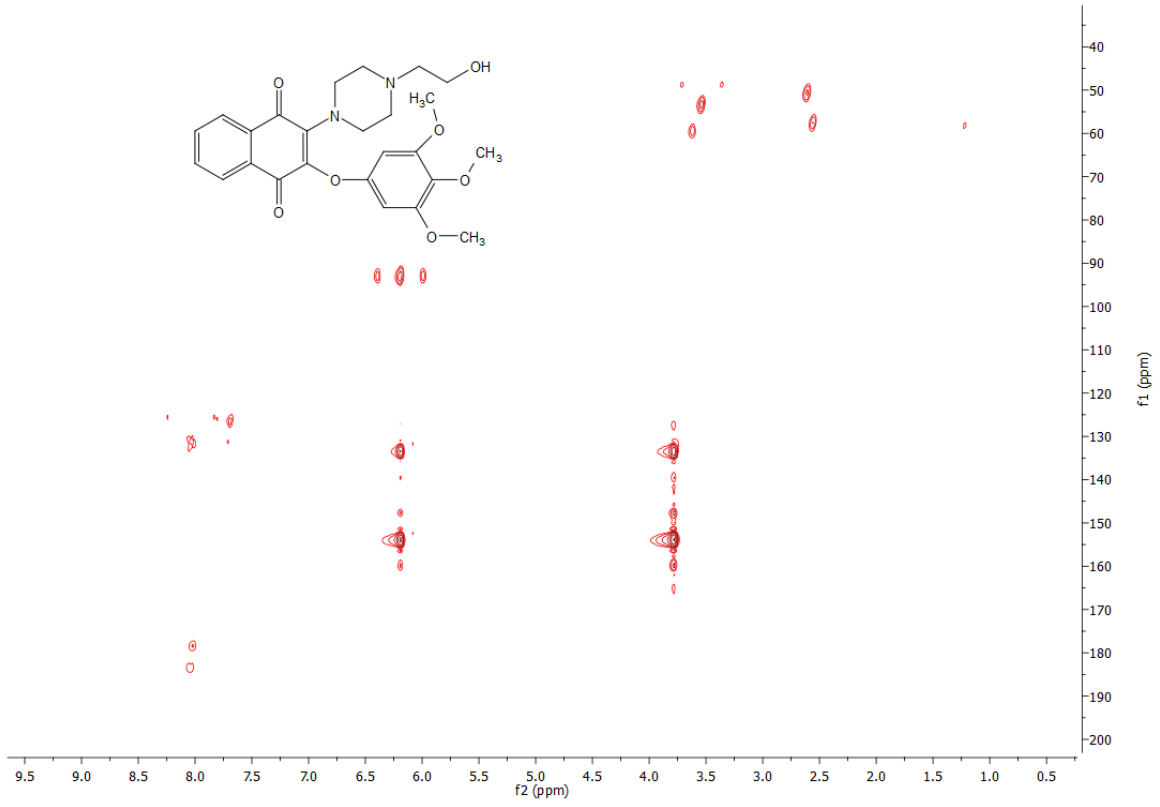

Figure S21. $^{1}H,^{13}C$ long range correlations by HMBC experiment (400MHz, $CDCl_3$) of **3.**

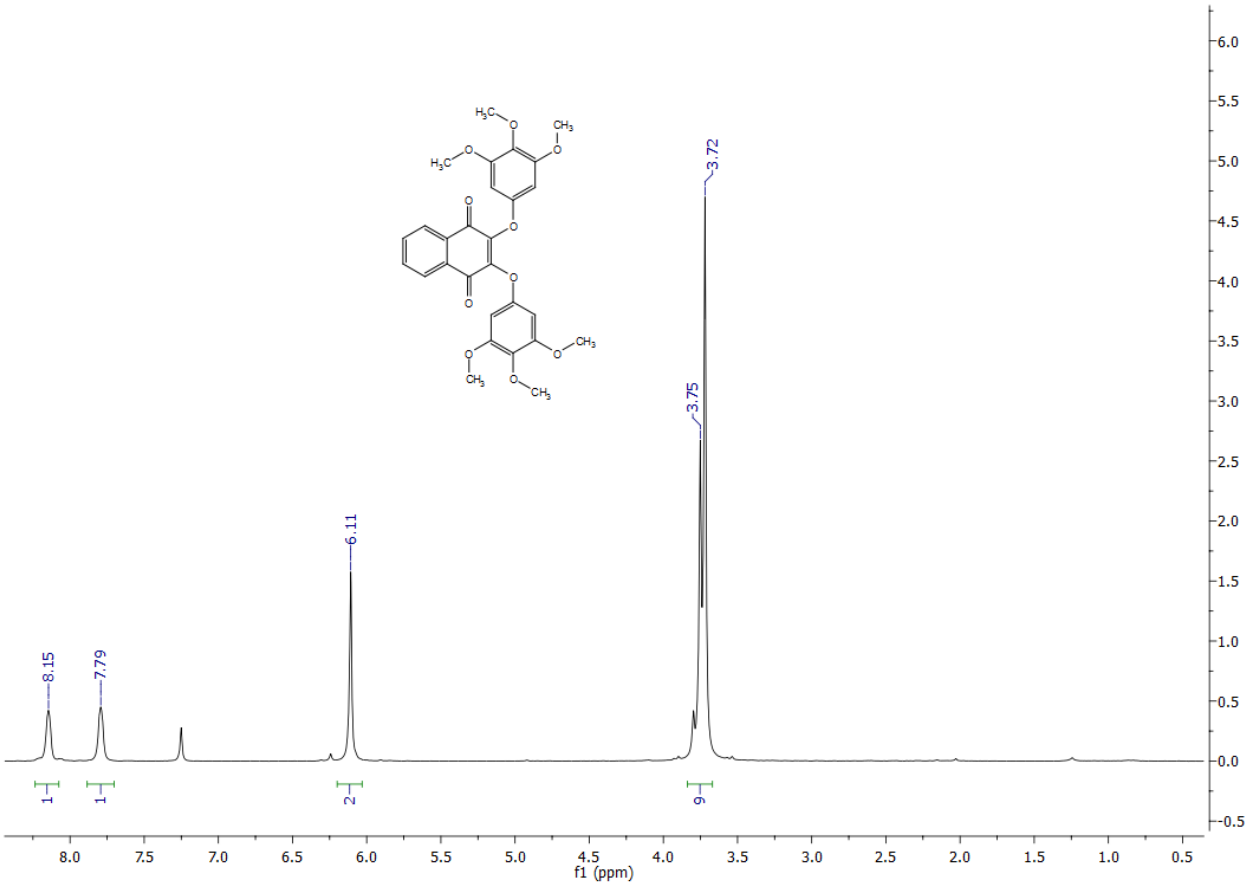

Figure S22. [1]HNMR spectrum (400MHz, $CDCl_3$) of precursor **4.**

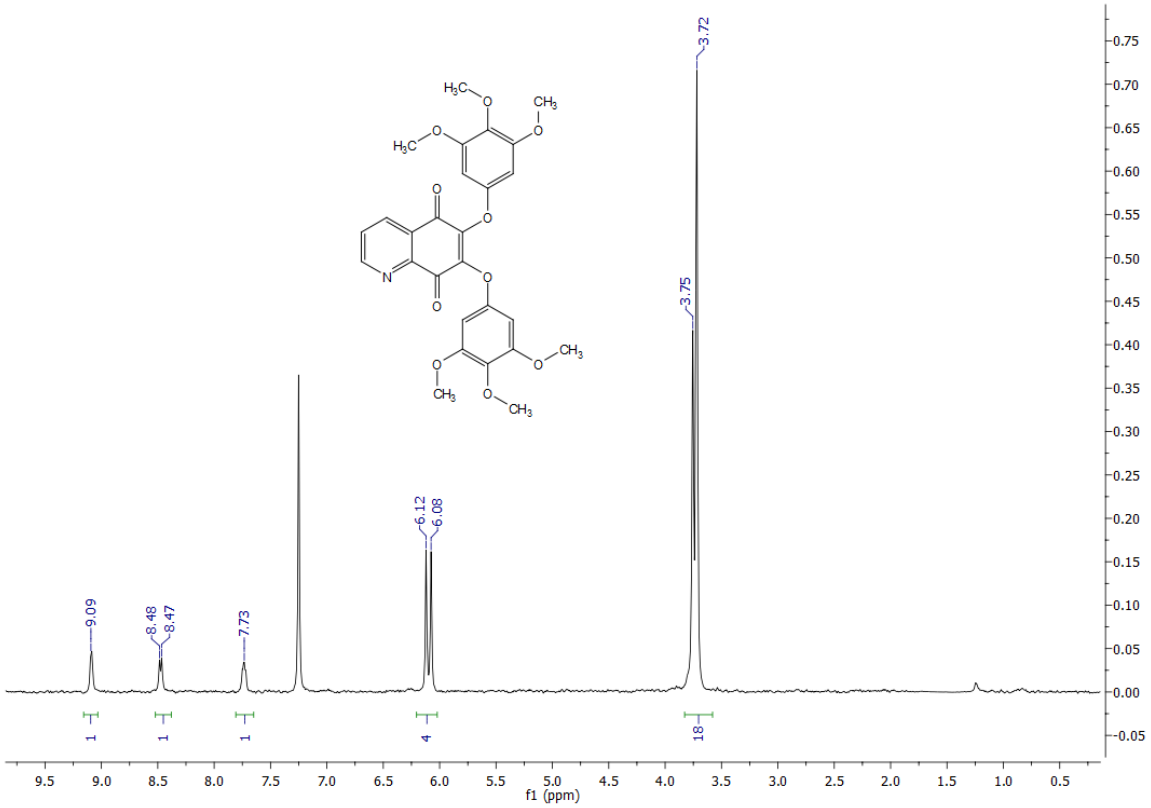

Figure S23. [1]HNMR spectrum (400MHz, $CDCl_3$) of precursor **5.**